Green catalytic reactions with high atom economy: oxidation of isoprene glycol, unsymmetric disulfane synthesis, polysulfane synthesis, and asymmetric aminolysis

河合, 靖貴

Green catalytic reactions with high atom economy: oxidation of isoprene glycol, unsymmetrical disulfane synthesis, polysulfane synthesis, and asymmetric aminolysis

Yasutaka KAWAI

Catalysis Organic Chemistry Laboratory

Department of Chemistry
Graduate School of Science
Kyushu University

January, 2022

General Introduction

Synthetic chemistry is indispensable to modern human society. It has a history of more than 100 years and has contributed to the development of human society by producing a variety of chemicals and materials from fossil resources and other sources. Until the mid-20th century, synthetic chemists focused on how to make products easily, in large quantities, and inexpensively. Environmental impact and safety were not recognized as important issues. However, problems have emerged such as environmental destruction, pollution, depletion of resources and energy, and accidents caused by explosives and toxic substances. In 1997, Paul T. Anastas and his colleagues compiled the 12 principles of green chemistry, which were published by the United States Environmental Protection Agency [1].

Green chemistry's 12 principles

1. Prevent waste: Design chemical syntheses to prevent waste. Leave no waste to treat or clean up.
2. Maximize atom economy: Design syntheses so that the final product contains the maximum proportion of the starting materials. Waste few or no atoms.
3. Design less hazardous chemical syntheses: Design syntheses to use and generate substances with little or no toxicity to either humans or the environment.
4. Design safer chemicals and products: Design chemical products that are fully effective yet have little or no toxicity.
5. Use safer solvents and reaction conditions: Avoid using solvents, separation agents, or other auxiliary chemicals. If you must use these chemicals, use safer ones.
6. Increase energy efficiency: Run chemical reactions at room temperature and pressure whenever possible.
7. Use renewable feedstocks: Use starting materials (also known as feedstocks) that are renewable rather than depletable. The source of renewable feedstocks is often agricultural products or the wastes of other processes; the source of depletable feedstocks is often fossil fuels (petroleum, natural gas, or coal) or mining operations.
8. Avoid chemical derivatives: Avoid using blocking or protecting groups or any temporary modifications if possible. Derivatives use additional reagents and generate waste.
9. Use catalysts, not stoichiometric reagents: Minimize waste by using catalytic reactions. Catalysts are effective in small amounts and can carry out a single reaction many times. They are preferable to stoichiometric reagents, which are used in excess and carry out a reaction only once.
10. Design chemicals and products to degrade after use: Design chemical products to break down to innocuous substances after use so that they do not accumulate in the environment.
11. Analyze in real time to prevent pollution: Include in-process, real-time monitoring and control during syntheses to minimize or eliminate the formation of byproducts.
12. Minimize the potential for accidents: Design chemicals and their physical forms (solid, liquid, or

gas) to minimize the potential for chemical accidents including explosions, fires, and releases to the environment.

In 2015, the 17 Sustainable Development Goals (SDGs) were adopted unanimously by the member states at the United Nations Summit [2]. These SDGs are an evolution and broadening of the scope of green chemistry. Nowadays, the concepts of green chemistry and SDGs have become principles that can no longer be ignored in the development of organic reactions.

In my doctoral research, the author has investigated four reactions that are useful for promoting green chemistry. All of them are catalytic reactions, and in that respect, they are consistent with Principle 9.

In Chapter 1, enantioselective aminolysis of azlactone with organic catalysts is described. Organic catalysts are consistent with Principles 1, 4, 7, and 9 of Green chemistry as catalysts that do not use potentially toxic and rare metals. Although aminolysis of azlactones is a highly atom efficient reaction for the synthesis of amino acid derivatives, very poor examples of asymmetric aminolysis of azlactones were reported. In this research, using *tert*-butyl carbazate as a nucleophile, the product was obtained in 42% yield with 69% ee. Notably, this product readily undergoes enantiomeric preferential enrichment. The product of about 70% ee can easily exceed 90% ee by crystallization of the racemic compound. Since this phenomenon led to inaccurate HPLC measurement results, scopes of alcohol, solvent, and catalyst need to be reconsidered for the future.

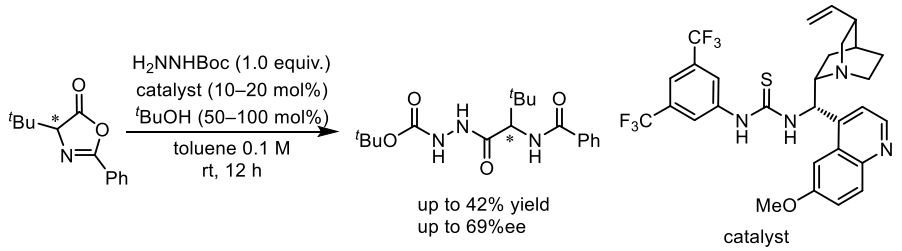

Scheme 1. Asymmetric aminolysis of azlactones with thiourea catalysts

Chapter 2 and later chapters dealt with syntheses using heterogeneous catalysts, which are considered more environmentally friendly. In chapter 2, an aerobic oxidation of isoprene glycol with platinum-bismuth nanoparticles supported on metal oxides to afford 3-hydroxy-3-methylbutanoic acid (HMB), which is a promising therapeutic agent preventing muscle breakdown or as a supplement for muscle building. Some of the reported synthetic methods for HMB use stoichiometric amounts of pyridine and iodine with low atomic efficiency. Aerobic oxidation with heterogeneous catalysts is consistent with Principles 1, 2, and 9 of green chemistry. The author was able to develop a catalyst with less leaching and sintering problems and better reusability than the previously reported activated carbon supported Pt-Bi catalysts.

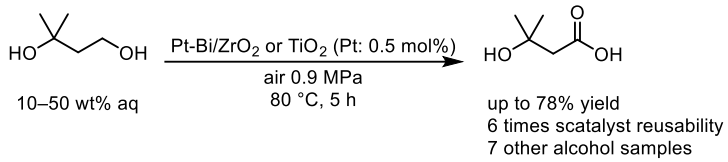

Scheme 2. Aerobic oxidation of isoprene glycol with supported Pt-Bi catalysts

In Chapter 3, a novel method for the synthesis of unsymmetrical disulfanes. The structures of unsymmetrical disulfane are often found in biologically active compounds, but there is no efficient synthetic method up to now. A simple method for synthesizing disulfanes, oxidative dimerization of thiols, is not practical because it produces three different compounds in statistical proportions. The method of thiol substitution on symmetrical disulfanes, which the author achieved in this study, is the simplest reaction, but a suitable method had not been reported because thiols themselves easily undergo oxidative dimerization. Therefore, most of the methods reported by other researchers so far are based on introducing a leaving group to one of the sulfanyl groups, which resulted in a very low atom efficiency. The reaction reported by the author is excellent in high atom efficiency as well as commercial available and inexpensiveness of the catalyst basic zeolites (MS-13X), which are not only easy to separate but also can be reused almost endlessly. This method is superior in terms of principles 1, 2, 5, 8, and 9 of green chemistry.

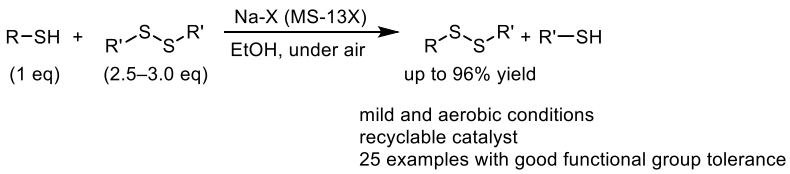

Scheme 3. Synthesis of unsymmetrical disulfanes by basic zeolite-catalyzed thiol-disulfane Exchange Reaction

In Chapter 4, the author described the novel synthesis of dialkylpolysulfanes from alkenes, elemental sulfur (S_8), and hydrogen. Dialkylpolysulfanes have been used as extreme-pressure additives and lubricating fluid compositions. These compounds are often used in the field of tribology, which is at the interface between mechanical and chemical engineering. The current production method for dialkylpolysulfanes employs hydrogen sulfide, alkenes, and elemental sulfur (S_8). Hydrogen sulfide is a highly toxic and dangerous compound, and it has been desired to develop a synthetic method that can avoid using it. The method reported by the author has a great advantage in that hydrogen can be used instead of hydrogen sulfide by developing new heterogeneous cobalt catalysts. The resulting polysulfane is to be a mixture of similar compositions to conventional products. It is excellent in terms of principles 3, 4, 9, and 12 of green chemistry.

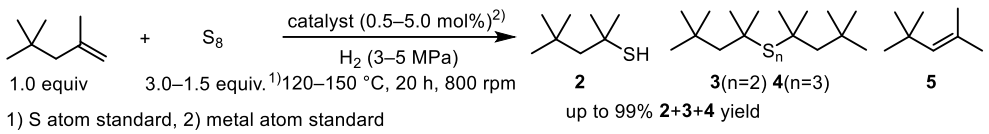

Scheme 4. Synthesis of dialkylpolysulfanes from alkenes, elemental sulfur (S8), and hydrogen catalyzed by heterogeneous cobalt catalysts.

In each chapter, the author describes the details of these studies and discusses the reaction mechanisms and future issues to be resolved.

References

[1] P.T. Anastas, T. C. Williamson, Green Chemistry, ACS Symposium Series; American Chemical Society: Washington, DC, 1996., 1 –17.

[2] *United Nations, Department of Economic and Social Affairs, Sustainable Development* (https://sdgs.un.org/)

Contents

Chapter 1. Enantioselective Aminolysis of Azlactone with Acid-Base Catalyst

Abstract

Asymmetric aminolysis of azlactone was developed by using thiourea acid-base catalysts. In this research, using *tert*-butyl carbazate as a nucleophile, the product was obtained in 42% yield with 69% ee. Notably, this product readily undergoes enantiomeric preferential enrichment. The product of about 70% ee can easily exceed 90% ee by crystallization of the racemic compound. Since this phenomenon led to inaccurate HPLC measurement results, scopes of alcohol, solvent, and catalyst need to be reconsidered for the future.

Introduction

Some useful small-molecule compounds, such as pharmaceuticals, have asymmetric centers derived from α-amino acids. One of the enantioselective synthesis methods for such skeletons is the asymmetric ring-opening reaction of azlactones synthesized from the corresponding α-amino acids. Asymmetric hydrolysis and alcoholysis of azlactones have already been reported [1.1-11]. On the other hand, very poor examples of asymmetric aminolysis were reported. Although Pascal and his co-workers reported asymmetric ring-opening reaction of azlactones using chiral amino acids, peptide compounds, or these derivatives as nucleophiles as one of the reactions using nitrogen atoms as nucleophiles, the maximum diastereomeric ratio was 80:20 [1.12]. Shi and co-workers reported catalytic asymmetric ring-opening aminolysis of azlactones with chiral phosphate catalysts (Scheme 1.1a) [1.13]. This reaction showed high yield and stereoselectivity, however, the diarylhydroxymethyl group was required for directing group. In addition, Shao and co-workers reported stereoselective ring-opening aminolysis of azlactone by indoline with chiral phosphate catalysts (Scheme 1.1b) [1.14]. Herein, this author investigated asymmetric azlactone ring-opening aminolysis with chiral acid-base catalysts. Asymmetric azlactone ring-opening reaction with acid-base catalysts had been reported in alcoholysis [1.3, 1.4]. That method was adapted to aminolysis in this report. Additionally, the products of this reaction were found to be prone to preferential enrichment. Therefore, the enantiomeric excess of products in Table 1.1-3 was not accurate.

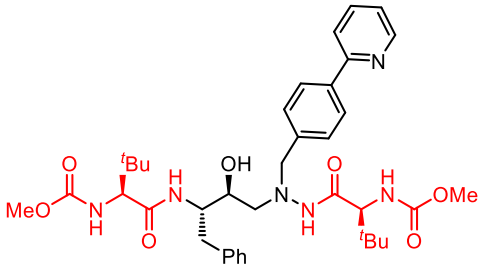

Atazanavir (HIV protease inhibitor)

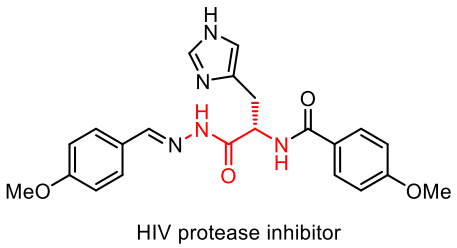

HIV protease inhibitor

Figure 1. 1. Amino acid derivative compounds

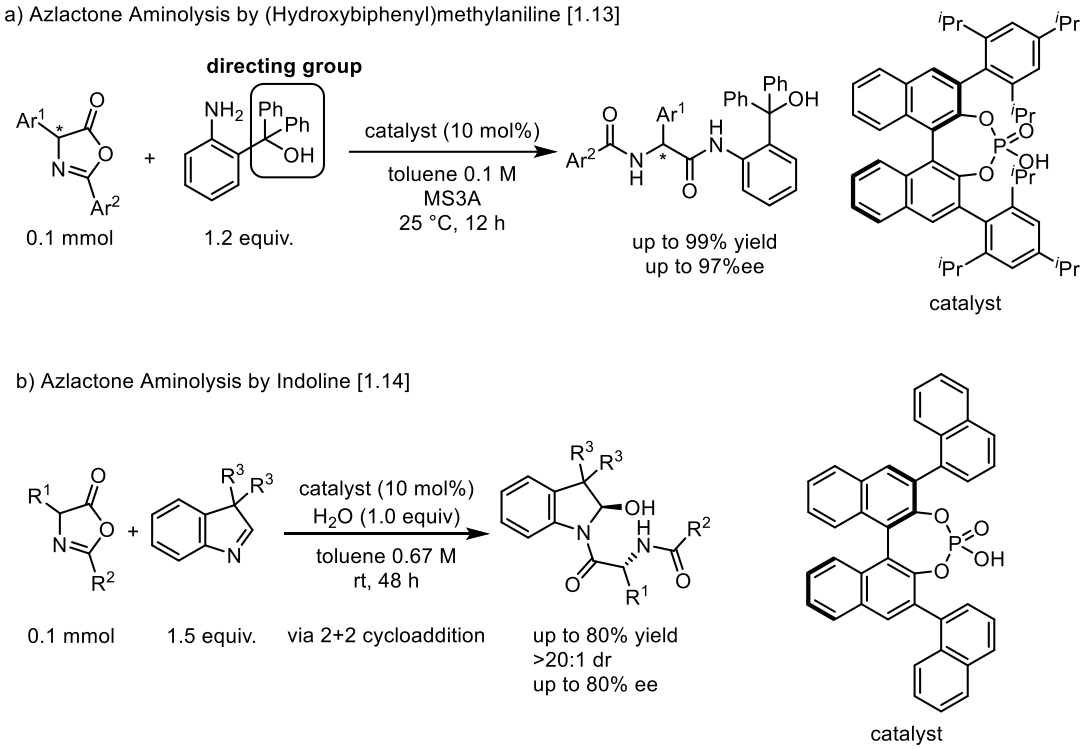

Scheme 1. 1. Previous report of azlactone aminolysis

Scope of Reaction Conditions

Initially, the author investigated the reaction conditions of aminolysis of azlactone. The author used *tert*-butyl carbazate as a nucleophile, acid-base catalyst **3a**, and ^{t}BuOH as an additive (Table 1.1 entry 1). The result was 40% conversion, 35% yield, and 93%ee. Using ^{i}PrOH as an additive showed a similar result of ^{t}BuOH (Table 1.1 entry 2). However, ^{t}AmylOH and 1-adamantanol gave increasing in yield and decreasing in ee (Table 1.1 entries 3 and 4). The heating reaction mixture also lead to decreasing in ee (Table 1.1 entry 5). From these results, the author determined ^{t}BuOH as an appropriate additive.

Table 1. 1. Scope of additive

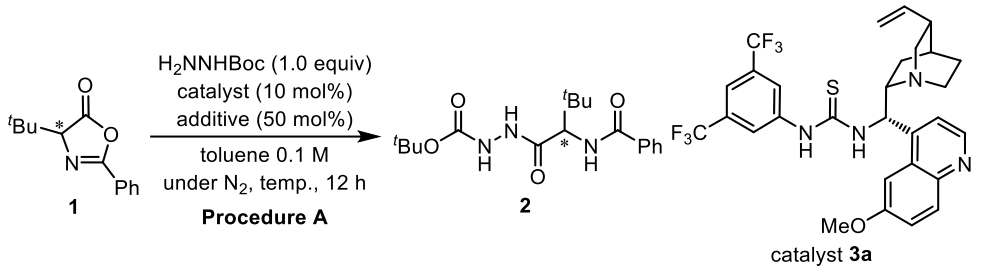

entry	additive	temperature	conv. (%)	yield (%)	ee (%)
1	^{t}BuOH	rt	40	35	93
2	^{i}PrOH	rt	47	32	94
3	^{t}AmylOH	rt	60	57	57
4	1-adamantanol	rt	66	71	26
5	^{t}BuOH	50 ºC	59	63	47

Using the selected additive, the author explored the solvent (Table 1.2). THF showed a slightly lower yield (29%) and ee (75%) (entry 2). Other ether solvents resulted in very low ee (entries 3 and 4). MeCN lead to much lower ee (entry 5) and $CHCl_3$ gave the racemic product (entry 6).

Table 1. 2. Scope of solvent.

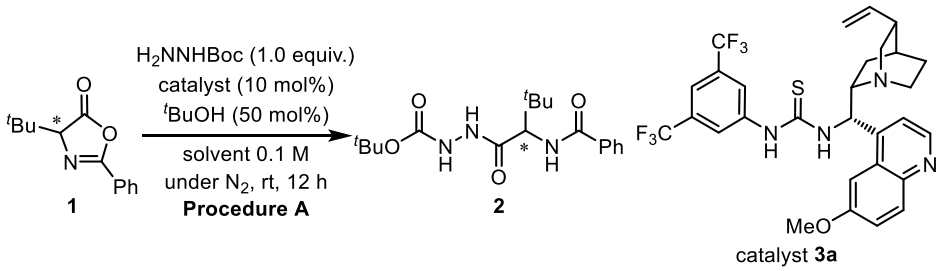

entry	solvent	conv. (%)	yield (%)	ee (%)
1	toluene	40	35	93
2	THF	38	29	75
3	1,4-dioxane	53	29	15
4	CPME	53	48	13
5	MeCN	34	33	9
6	$CHCl_3$	78	77	0

Under the determined conditions, the author investigated the effect of the structure of acid-base catalysts (Table 1.3). Initially, the chirality of the 9th carbon in quinine structure was presumed to determine the stereochemistry of the product. However, enantiomeric excess of the product of the

reaction with catalyst **3b**, which is a diastereomer with different stereochemistry of the 9th carbon of **3a**, was very poor and the enantioselectivity was the same as that of the reaction with **3a** (entry 2). Therefore, the stereochemistry of the 8th carbon in quinine structure was also investigated. Then, another enantiomer was obtained with middle ee when catalyst **3d**, which has different stereochemistry at both the 8th and 9th carbon, was used (entry 4). The results showed stereochemistry of the two asymmetric carbons in the catalyst is important for the enantioselectivity of the product. In addition, the structure of the base site was investigated and these catalysts gave low enantiomeric products (entries 5-7). Interestingly, the stereochemistry of the major enantiomer of the product of the reaction with **3f** or **3g** was inverted even though they have the same conformation.

Table 1. 3. Scope of catalyst

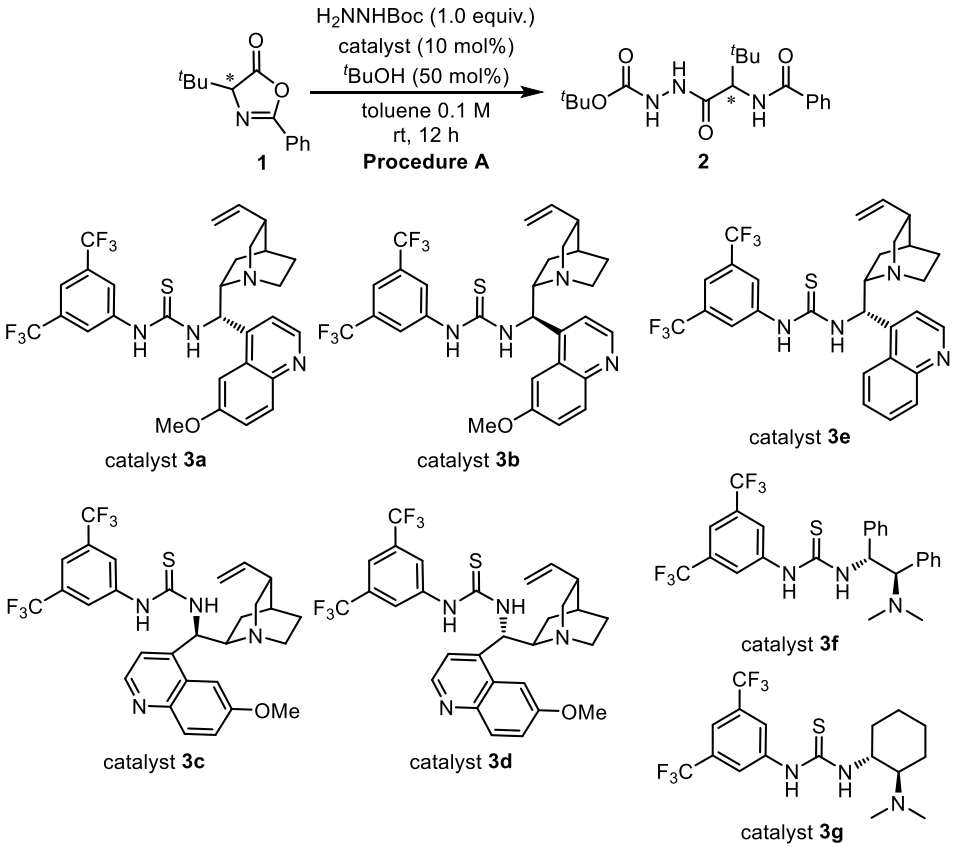

entry	catalyst	conv. (%)	yield (%)	ee (%)
1	**3a**	40	35	93
2	**3b**	67	49	6
3	**3c**	66	66	-9
4	**3d**	17	16	-63
5	**3e**	75	65	28
6	**3f**	46	42	-28
7	**3g**	63	48	44

Next, the author tried to find out why the results were shown in Table 1.1–3 sometimes gave products over 90% ee and sometimes gave much lower ee. As a result, the author found that this product readily undergoes enantiomeric preferential enrichment [1.15]. The product of about 70% ee can easily exceed 90% ee by crystallization of the racemic compound. The author was even able to clarify that the very easy formation of racemate crystals was the cause. Measurement of the ee of the crystals readily obtained from the product shows that it is racemic (0% ee), which is thought to cause preferential enrichment.

Since the product was crystallized selectively as racemic material and preferential enrichment was occurring, the reaction conditions were explored again (Table 1.4). The reaction in the first condition was performed in procedure B to give product **2a** in 37% yield and 69%ee (entry 1). Then, the amount of the alcohol was increased to 100 mol%, or alcohol dehydrated by molecular sieves was used. However, the yield was only slightly reduced and the ee was kept at 69% in each case. In addition, increasing the catalyst **3a** to 20 mol% showed slightly increasing the yield of **2a** and keeping the ee 69%.

Table 1. 4. Scope of reaction conditions

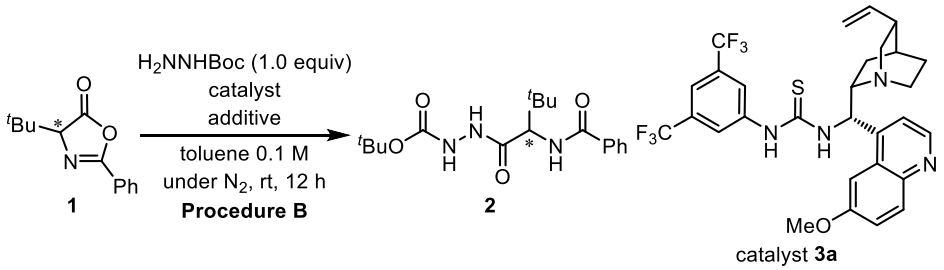

entry	catalyst (mol%)	additive	conv. (%)	yield (%)	ee (%)
1	10	^{t}BuOH 50 mol%	34	37	69
2	10	^{t}BuOH 100 mol%	28	25	69
3	10	dried ^{t}BuOH 50 mol%	28	26	69
4	20	^{t}BuOH 50 mol%	37	42	69

Conclusions

In conclusion, we established aminolysis of azlactone in middle enantiomeric excess. The enantioselectivity was controlled by the stereochemistry of the catalyst. Preferential enrichment of enantiomer was observed in this product. In the future, it is expected to improve the yield and enantioselectivity, and to expand the range of substrate applications.

General Procedures

Procedure A

Air in 10 mL screw vial containing azlactone, screw vial containing carbazate ester, and screw vial containing catalyst were replaced with N_2. 0.3 mL solvent was added into azlactone vial, 0.5 mL solvent was added into carbazate ester vial, and 0.2 mL solvent was added into catalyst vial. Catalyst solution and ^{t}BuOH were added into azlactone vial. Carbazate ester solution was added to the mixture at last. The reaction solvent was stirred predetermined time then removed catalyst with a short column. The mixture was concentrated and dried under reduced pressure. The residue was purified by flash column chromatography (45 mL SiO_2, 1:1 hexane-Et_2O 150 mL—Et_2O 100 mL).

Procedure B

Azlactone and catalyst were put into a 10 mL screw vial. Carbazate ester was put into another screw vial. Air in these vials was replaced with N_2. 0.5 mL solvent was added to each vial. ^{t}BuOH was added a mixture of azlactone and catalyst. The mixture was stirred for 15 min then carbazate ester solution was added to the mixture at last. The reaction solvent was stirred predetermined time then was purified by flash column chromatography (45 mL SiO_2, 1:1 hexane-Et_2O 150 mL—Et_2O 100 mL).

References

[1.1] For a review, see; P. P. de Castro, A. G. Carpanez and G. W. Amarante, Chem. Eur. J. 2016, 22, 10294–10318

[1.2] Y.-C. Zhang, Q. Yang, X. Yang, Q.-N. Zhu and F. Shi, Asian J. Org. Chem. 2016, 5, 914 –919.

[1.3] A. Berkessel, F. Cleemann, S. Mukherjee, T. N.Müller, and J. Lex, Angew. Chem. Int. Ed. 2005, 44, 807–811.

[1.4] A. Berkessel, S. Mukherjee, F. Cleemann, T. N.Müller, and J. Lex, Chem. Commun. 2005, 1898–1900.

[1.5] A. Peschiulli, C. Quigley, S. Tallon, Y. K. Gun'ko, S. J. Connon, J. Org. Chem. 2008, 73, 6409–6412.

[1.6] J. W. Lee, T. H. Ryu, J.S. Oh, H. Y. Bae, H. B. Jang, C. E. Song, Chem. Commun. 2009, 7224–7226.

[1.7] G. Lu, V. B. Birman, Org. Lett. 2011, 13, 356–358.
[1.8] S. Tallon, F. Manoni, S. J.Connon, Angew. Chem. Int. Ed. 2015, 54, 813–817.
[1.9] H. Mandai, K. Hongo, T. Fujiwara, K. Fujii, K. Mitsudo, S. Suga, Org. Lett. 2018, 20, 4811–4814.
[1.10] M. S. Xie, B. Huang, N. Li, Y. Tian, X. X. Wu, Y. Deng, G. R. Qu, H. M. Guo, J. Am. Chem. Soc. 2020, 142, 19226–19238.
[1.11] K. Wakafuji, S. Iwasa, K. N. Ouchida, H. Cho, H. Dohi, E. Yamamoto, T. Kamachi and M. Tokunaga, Acs Catal. 2021, 11, 14067–14075.
[1.12] D. Beaufils, G. Danger, L. Boiteau, J.-C. Rossi, and R. Pascal, Chem. Commun. 2014, 50, 3100–3102.
[1.13] Y.-C. Zhang, Q. Yang, X. Yang, Q.-N. Zhu, and F. Shi, Asian J. Org. Chem. 2016, 5, 914–919.
[1.14] D. J. Cheng, R.-Q. Li, L. Boiteau, X.-S. Zhang, L. Zhao, T. Wang and Y.-D. Shao, Eur. J. Org. Chem. 2016, 5, 914–919.
[1.15] a) S. Iwama, M. Horiguchi, H. Sato, Y. Uchida, H. Takahashi, H. Tsue, and R. Tamura, Cryst. Growth Des., 2010, 10, 2668–2675. b) R.Tamura, H. Takahashi, T. Ushio, J. Synth. Org. Chem. Jpn. 1998, 56, 38–49. c) K. Kinbara, K. Saigo, Journal of the Crystallographic Society of Japan. 1996, 38, 414–420.

Chapter 2. Aerobic Oxidation of Isoprene glycol with Platinum-Bismuth Alloy Supported on Metal Oxide

Abstract

A metabolite of leucine, 3-hydroxy-3-methylbutanoic acid (HMB) is expected as a promising therapeutic agent preventing muscle breakdown or as a supplement for muscle building. For industrial production of HMB, Pt-catalyzed base-free aerobic oxidation of isoprene glycol, which is one of the inexpensive feedstocks, is a potent synthetic method for providing HMB. However, the previous report on the aerobic oxidation of isoprene glycol with Pt-Bi supported on activated carbon catalyst suffered from low tolerance to high substrate concentration conditions, which leads to low volumetric productivity. Herein, the author reported base-free aerobic oxidation of isoprene glycol using Pt-Bi bimetallic nanoparticles (NPs) supported on ZrO_2 or TiO_2 as a catalyst, showing high tolerance to the reaction conditions with a high concentration of alcohol substrate. In addition, these catalysts also exhibited high recyclability. Scanning transmission electron microscopy analyses suggested that the Pt-Bi NPs supported on ZrO_2 or TiO_2 are less likely to aggregate Pt and Bi species than that NPs supported on activated carbon. Additionally, these catalysts showed lower leaching after catalyst recycling.

Introduction

A metabolite of leucine, 3-hydroxy-3-methylbutanoic acid (HMB) has received considerable attention because of the effect of suppressing muscle loss [2.1] and is expected as a promising therapeutic agent preventing muscle breakdown [2.2, 2.3] or as a supplement for muscle building [2.4]. Various industrial synthetic methods of HMB have been developed such as oxidation of diacetone alcohol with iodine followed by base hydrolysis [2.5], oxidation of diacetone alcohol with sodium hypochlorite [2.6], base hydrolysis of 4,4-dimethyloxetane-2-one [2.7], or 1,2-addition of activated acetyl compounds to acetone using biocatalysts (Scheme 2.1a–d) [2.8]. The oxidation of acetone dimer has been reported using iodine and sodium hypochlorite as oxidants. However, the former produces an equivalent amount of iodine and pyridine, while the latter produces a waste product derived from sodium hypochlorite, and the sodium ion must be removed with hydrochloric acid at the end. The ring-opening reaction of oxetanone does not produce oxidant-derived byproducts, but again requires removal of sodium ions with hydrochloric acid at the end. The enzymatic reaction requires an acetyl compound with a leaving group and is therefore less atomically efficient. In this way, these methods have problems such as the need to remove sodium ions, the need for an equivalent amount of oxidant, and the formation of by-products. Therefore, they are not suitable for industrialization. Among them, the aerobic oxidation of isoprene glycol (IPG), which is one of the chemical feedstocks, using a supported Pt-Bi catalyst was devised as an industrial production method for HMB (Scheme 2.1e). Since air is used as the oxidizing agent in this reaction, the only byproduct derived from the oxidizing

agent is water, which is used as a solvent, and virtually no byproducts are produced. Another advantage is that the catalyst is solid, so it is easy to reuse. Furthermore, since HMB is obtained as is, there is no need to treat it with hydrochloric acid after the reaction.

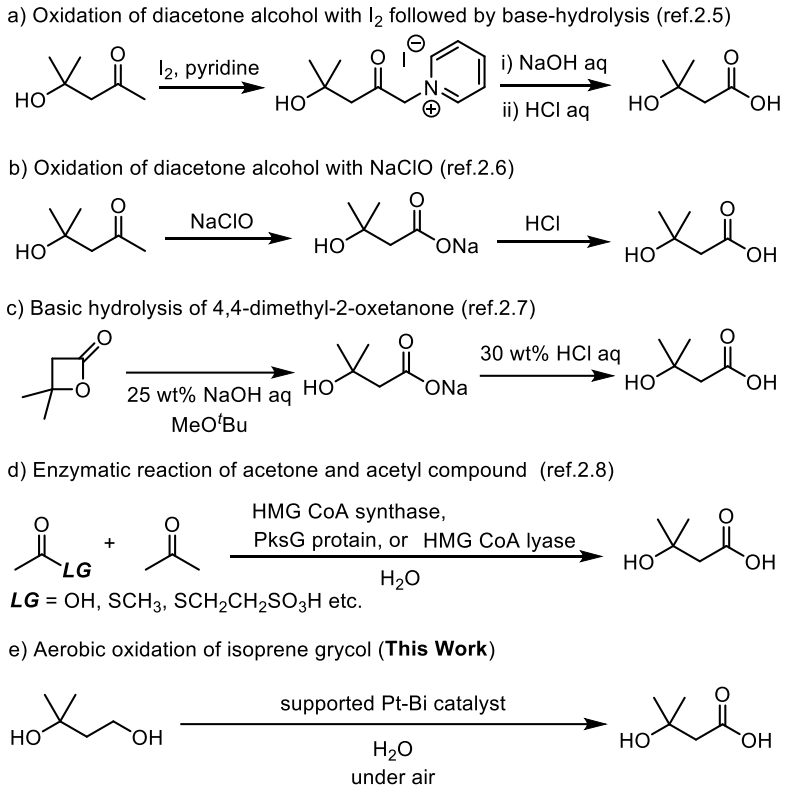

Scheme 2. 1. Method of HMB synthesis

Supported metal nanoparticle catalysts such as Pt, Pd, and Au have been generally employed for the oxidation of alcohols by O_2 gas or air [2.9-2.12]. In particular, Pt or Pt-Bi catalysts are superior in that the reaction proceeds without bases. Effects of Bi are activating platinum by donating electrons, preventing platinum poisoning, and providing sacrificial oxidation. An activated carbon-supported Pt-Bi catalyst was also employed for the aerobic oxidation of IPG in a patent [2.13]. However, there exist several issues that remain to be solved. For example, activated carbon-supported Pt catalysts generally have low reusability when used in the aerobic oxidation of alcohols [2.14]. In addition, various side reactions such as acetalization of the aldehyde intermediate with IPG and dehydration of aldehyde intermediate or HMB would potentially proceed under the reaction conditions for aerobic oxidation of IPG. Nevertheless, the details of the reaction path have remained unexplored. Furthermore, performing the reaction at a higher substrate concentration is desirable since the volumetric productivity is important in terms of the efficiency of the industrial processes while high substrate concentration increases byproducts and decreases selectivity for carboxylic acids in aerobic oxidation

of alcohols with a metal catalyst [2.15]. However, the effect of substrate concentration in aerobic oxidation of alcohols with heterogeneous catalysts has not been investigated enough. Moreover, HMB has high water solubility and requires a lot of energy to purify the product from water. Taking these issues into consideration, the mechanistic investigation of aerobic oxidation of IPG and the development of new heterogeneous Pt catalysts having high activity and recyclability at high substrate concentrations are important goals from the viewpoint of green chemistry. Our group has been dedicated to the development of reactions with transition-metal nanoparticles (NPs) catalysts supported on metal oxides [2.16]. The metal-support interactions in the heterogeneous catalysts often affect the catalytic activity, selectivity, and reusability. Hence, metal oxide supports have recently gathered much attention as a handle for improving catalytic performances [2.17]. We envisioned that the use of appropriate metal oxide supports influences on the catalysis, which leads to improving the catalyst recyclability and the tolerance to the high substrate concentration conditions. Herein, we report that Pt-Bi nanoparticles catalysts supported on monoclinic ZrO_2 or rutile TiO_2 show high activity and recyclability in the aerobic oxidation of IPG in conjunction with the effect of the substrate concentrations. In addition, the results of several control experiments revealed the reaction pathways for side reactions of intermediates and byproducts.

General Procedures

General Procedure for the Preparation of Supported Pt-Bi Catalyst

The metal oxide support (MO_x, 969.3 mg) was impregnated with the aqueous solution of H_2PtCl_6 (1 mL, 20 g/L of Pt), and was heated at 40 °C with stirring until it become a powder. After that, the mixture was dried at 120 °C overnight, then calcined in air at 400 °C for 4 h to give the powder of calcined Pt/MO_x. The temperature in the calcination process was raised at a speed of 6.25 °C/min. $Bi(NO_3)_3{\cdot}5H_2O$ (24.9 mg, Bi 0.5 eq/Pt) was dissolved in HNO_3 aq (1 mol/L, 1 mL), and added to the calcined Pt/MO_x. The resulting mixture was heated at 40 °C with stirring until it became a powder and then dried at 120 °C overnight. The resultant powder was reduced with H_2 gas (20 mL/min) at 350 °C for 4 h to provide 2 wt% Pt-Bi/MO_x. The temperature in the reduction process was raised at a speed of 7.8 °C /min. After the reduction, the catalyst was cooled to room temperature. H_2 gas was replaced with N_2 gas before opening the oven.

In the case of the activated carbon-supported catalyst, the activated carbon (Maxsorb MSC-30) (969.3 mg) was impregnated with the solution of $Bi(NO_3)_3{\cdot}5H_2O$ (24.9 mg, Bi 0.5 equiv./Pt) in HNO_3 aq. (5 mL) and heated at 40 °C with stirring until it became a powder. After that, the mixture was dried at 120 °C overnight then impregnated with the aqueous solution of $Pt(NH_3)_4(NO_3)_2$ (5 mL of 7.94 g/L aqueous solutions). The resulting mixture was heated at 40 °C with stirring until it became a powder and then dried at 120 °C overnight. The resultant powder was reduced with H_2 gas (20 mL/min) at 350 °C for 4 h to provide 2 wt% Pt-Bi/C. The temperature in the reduction process was raised at a

speed of 7.8 °C /min. After the reduction, the catalyst was cooled to room temperature. H_2 gas was exchanged for N_2 gas before opening the oven. Note that the Pt loading was fixed at 2 wt% unless otherwise stated.

Catalyst Characterization

Particle sizes of Pt-Bi were determined by the combination of bright-field scanning transmission electron microscope images and CO adsorption measurements. Scanning Transmission Electron Microscope (STEM) and energy dispersive X-ray spectroscopy (EDS) were performed using a JEOL JEM-ARM200F microscope operated at 200 kV. CO-pulse adsorption was performed using BEL JAPAN INC. BELCAT-MS. The overall catalyst structure was investigated by powder X-ray diffraction (XRD) conducted on a Rigaku MiniFlex600 equipped with a Cu *Kα* radiation source. The supported metal amounts in the prepared or used catalysts were determined by microwave plasma atomic emission spectroscopy (MP-AES) using an Agilent 4100 system. The properties of the surface species of Pt and Bi were analyzed by X-ray photoelectron spectroscopy (XPS) using PHI Quantera SXM equipped with an Al Kα radiation source at a pressure below 10^{-6} Pa order. The obtained binding energies were calibrated to the C1s peak at 284.8 eV [18]. XPS profiles were further analyzed using XPSPEAK41 software.

Optimization of Reaction Conditions

The Pt-Bi catalyst (0.5 mol% as Pt) and an aqueous solution of IPG (1.0 mmol, 10 wt%) were put into a 40 mL autoclave equipped with a magnetic stirrer bar. The autoclave was filled with 0.9 MPa of air and heated to 80 °C. The reaction mixture was stirred at 800 rpm for 5 hours. After that, the autoclave was cooled to 0 °C in an ice bath. Then, the reaction mixture was diluted with methanol and transferred to a screw vial. The screw vial was centrifuged, and the supernatant was collected. Methanol was added to the screw vial with the remaining catalyst, centrifuged, and the supernatant was collected. These processes were repeated three times, and all the supernatants were combined. To the resultant mixture was added diglyme (32.8 mg) as an internal standard for GC analysis. The mixture was analyzed by GC. After being concentrated under reduced pressure, the concentrated mixture was then analyzed by ^{1}H NMR using 2-methoxynaphtalene as an internal standard.

IPG Concentration Experiment

The Pt-Bi catalyst (0.5 mol% Pt), an aqueous solution of IPG (1.0 mmol of 10 wt% aq, 2.0 mmol of 20 wt% aq, 3.0 mmol of 30 wt% aq, or 5.0 mmol of 50 wt% aq) were put into a 40 mL autoclave equipped with a magnetic stirrer bar. The autoclave was connected to a 200 mL autoclave, and the volume of the system was adjusted by adding the water to keep the same O_2 equivalent. The autoclaves were filled with 0.9 MPa of air and heated to 80 °C. The reaction mixture was stirred at 900 rpm for 12 hours. After that, the autoclave was cooled to 0 °C in an ice bath. Then, the reaction mixture was diluted with methanol and transferred to a screw vial. The screw vial was centrifuged, and the supernatant was collected. Methanol was added to the screw vial with the remaining catalyst,

centrifuged, and the supernatant was collected. These processes were repeated three times, and all the supernatants were combined. To the resultant mixture was added diglyme (32.8 mg) as an internal standard for GC analysis. The mixture was analyzed by GC. After being concentrated under reduced pressure, the concentrated mixture was then analyzed by ^{1}H NMR using 2-methoxynaphtalene as an internal standard.

Catalyst Recycle Experiment

The Pt-Bi catalyst (0.5 mol% as Pt) and an aqueous solution of IPG (2.0 mmol, 20 wt%) were put into a 40 mL autoclave equipped with a magnetic stirrer bar. The autoclave was filled with 0.9 MPa of air and heated to 80 °C. The reaction mixture was stirred at 900 rpm for 12 h. After that, the autoclave was cooled to 0 °C in an ice bath. Then, the reaction mixture was diluted with methanol and transferred to a screw vial. The screw vial was centrifuged, and the supernatant was collected. Methanol was added to the screw vial with the remaining catalyst, centrifuged, and the supernatant was collected. These processes were repeated three times, and all the supernatants were combined. To the resultant mixture was added diglyme (32.8 mg) as an internal standard for GC analysis. The mixture was analyzed by GC. After being concentrated under reduced pressure, the concentrated mixture was then analyzed by ^{1}H NMR using 2-methoxynaphtalene as an internal standard. The removed catalyst was dried under reduced pressure then reused for the same reaction another five times. After the last reaction, the used catalyst was characterized by TEM, MP-AES, and XPS (only Pt-Bi/ZrO_2).

Results and Discussions

We initially screened Pt-Bi NPs catalysts supported on various metal oxides in the aerobic oxidation of IPG (Table 2.1). The catalyst supported on activated carbon gave HMB in 53% yield (entry 1). The catalysts supported on SiO_2 and γ-Al_2O_3 gave HMB in low yields (entries 2 and 3). The catalyst supported on rutile TiO_2 (Pt-Bi/TiO_2) gave HMB in high yield (77%) (entry 4). The catalyst supported on monoclinic ZrO_2 (Pt-Bi/ZrO_2) also gave HMB in high yield (entry 5). Next, we investigated the effect of the Pt: Bi ratio. The HMB yield of Pt-Bi/ZrO_2 (Pt: Bi = 1:1 molar ratio) catalyst, Pt-Bi/ZrO_2 (Pt: Bi = 4:1 molar ratio) catalyst and Pt/ZrO_2 (no Bi) catalyst were slightly lower than that of the Pt-Bi/ZrO_2 (Pt: Bi = 2:1 molar ratio) catalyst (entries 6–8). Based on these results, the 2 wt%Pt-1.07 wt%Bi (Pt: Bi = 2:1 molar ratio) catalysts supported on ZrO_2, or TiO_2 were selected as the suitable catalyst.

Table 2. 1. Optimization of reaction conditions for the oxidation of IPG

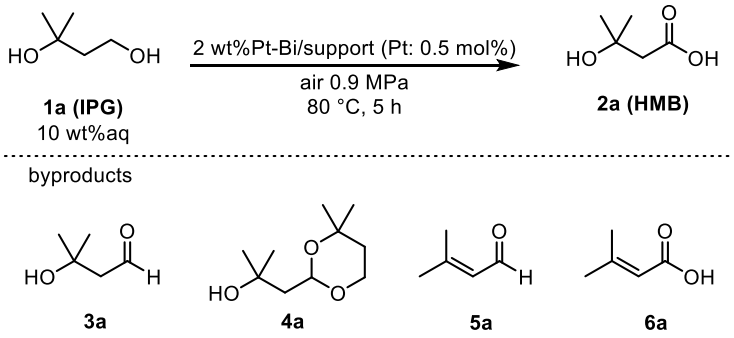

entries	support	Pt:Bi (molar ratio)	conv. (%)	yield (%)				
				2a	**3a**	**4a**	**5a**	**6a**
1	activated carbon[1)]	2:1	92	53	10	8	8	<1
2	SiO_2	2:1	61	21	24	10	3	<1
3	γ-Al_2O_3	2:1	83	25	19	5	13	<1
4	TiO_2[2)]	2:1	95	77	14	1	6	<1
5	ZrO_2[3)]	2:1	94	67	16	3	5	<1
6	ZrO_2[3)]	1:1	89	51	13	1	3	<1
7	ZrO_2[3)]	4:1	88	58	14	4	2	<1
8	ZrO_2[3)]	Pt only	96	55	22	2	4	1

1) Maxsorb MSC-30, 2) rutile type, 3) monoclinic form

The two Pt-Bismuth catalysts, which gave higher yields of HMB than the activated carbon support, were characterized in several ways. First, the crystalline state of the metal particles was confirmed by XRD (Figures 2.1-3). However, only the peaks of the support were observed and no information on the crystalline state of the supported metal particles could be obtained. Based on this observation, the metal particles were expected to be supported as nanoparticles, which were difficult to observe by XRD.

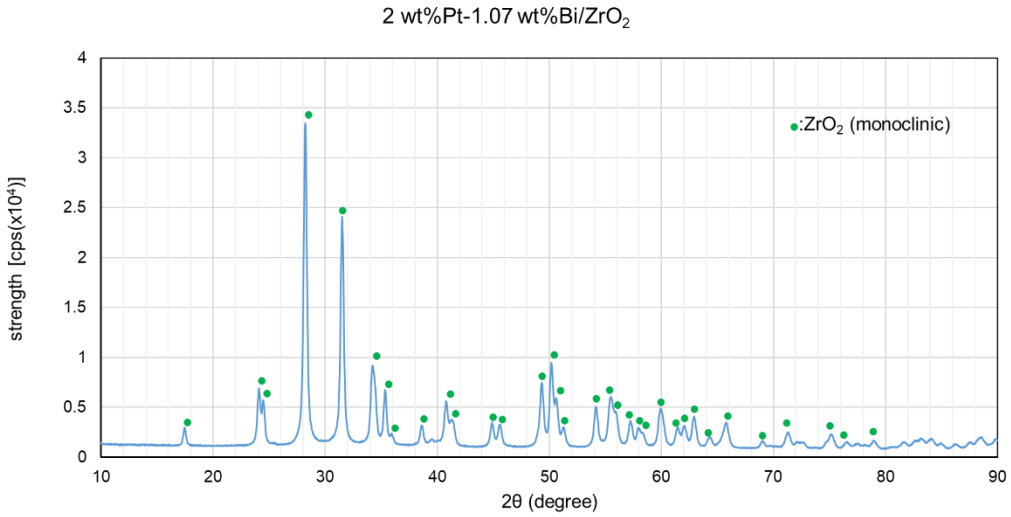

Figure 2. 1. XRD pattern of Pt-Bi/ZrO_2 catalyst

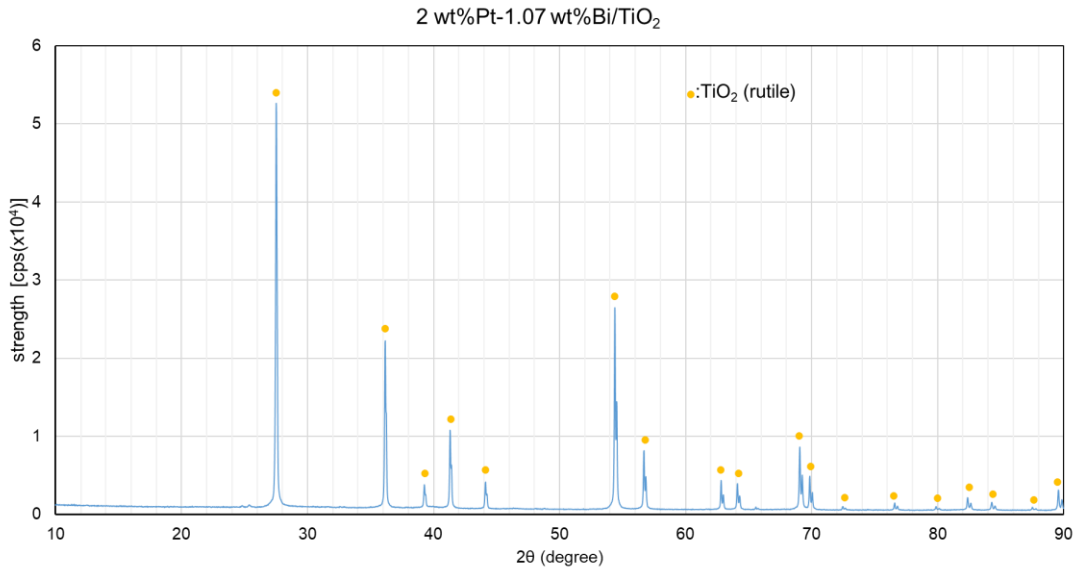

Figure 2. 2. XRD pattern of Pt-Bi/TiO_2 catalyst

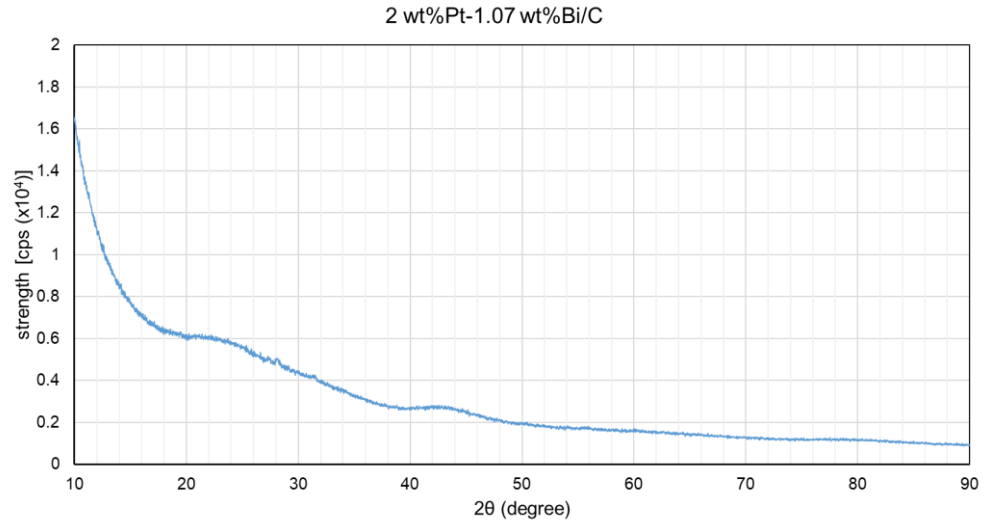

Figure 2. 3. XRD pattern of Pt-Bi/C catalyst

To confirm this prediction, the particle size of platinum-bismuth particles was measured (Figure 2.4). BF-STEM images of the catalysts show that nanoparticles on these catalysts are distributed. The average particle size of these catalysts was 2.2±1.0 nm (Pt-Bi/ZrO_2), 2.1±0.9 nm (Pt-Bi/TiO_2), and 1.4±0.4 nm (Pt-Bi/C). From these results, the supported metals were confirmed to be nanoparticles.

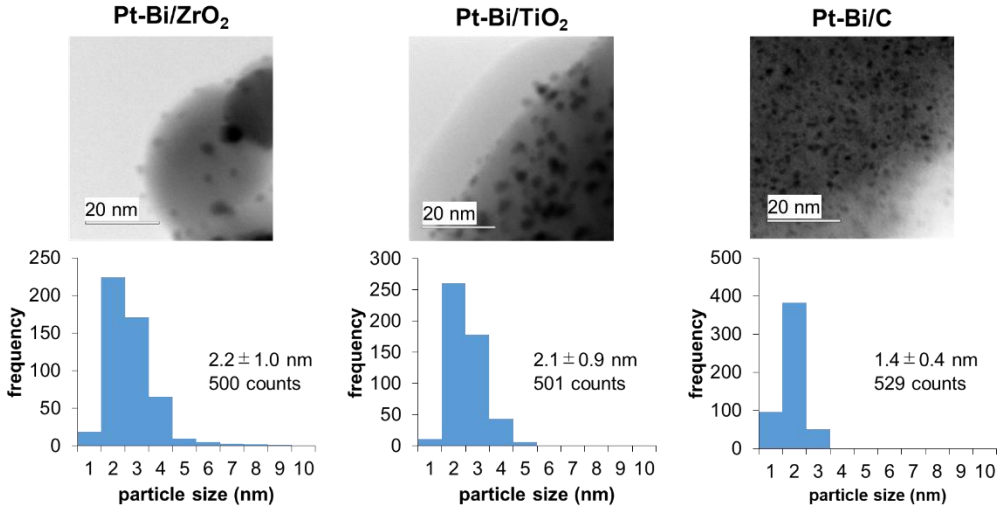

Figure 2. 4. BF-STEM images and average particle size of Pt-Bi catalysts

On the other hand, the average particle size measured by CO-pulse adsorption was 2.2 nm (Pt-Bi/ZrO_2), 5.6 nm (Pt-Bi/TiO_2), and 2.9 nm (Pt-Bi/C) (Table 2.2). In the case of the Pt-Bi/ZrO_2 catalyst, the particle sizes based on the CO-pulse adsorption analyses are in good agreement with those based on the TEM images, while slightly larger NPs sizes were suggested by the results of CO-pulse adsorption

analyses for the Pt-Bi/TiO_2 and Pt-Bi/C catalysts. The slight discrepancy in the particle sizes evaluated based on the TEM and CO-pulse adsorption was attributed to the difference in the surface state of the metal nanoparticles. Pt and Bi differ in their ability to adsorb CO molecules. Pt adsorbs CO molecules, while Bi has almost no ability to adsorb CO molecules [2.19]. Therefore, the more Bi there is on the surface of the metal nanoparticles, the larger particle size was measured by the CO pulse adsorption method compared with the particle size measured by STEM images. Hence, more Bi atom exists on the surface of the metal nanoparticles supported on TiO_2 and activated carbon compared with nanoparticles supported on ZrO_2.

Table 2. 2. Average particle size of Pt-Bi/ZrO_2, Pt-Bi/TiO_2, and Pt-Bi/C fresh catalysts measured by TEM observation and CO-pulse adsorption

catalyst	particle size (nm)	
	TEM	CO-pulse adsorption
Pt-Bi/ZrO_2	2.2±1.0	2.2
Pt-Bi/TiO_2	2.1±0.9	5.6
Pt-Bi/C	1.4±0.4	2.9

Both Pt and Bi on the catalyst were confirmed to be dispersed in the EDS analysis of Pt Lα and Bi Lα (Figures 2.5 and 2.6). When the larger particles in these catalysts were analyzed, Pt and Bi were observed at the location of the same particles. These results indicated a mixed nanoparticle of Pt and Bi was formed on these supports.

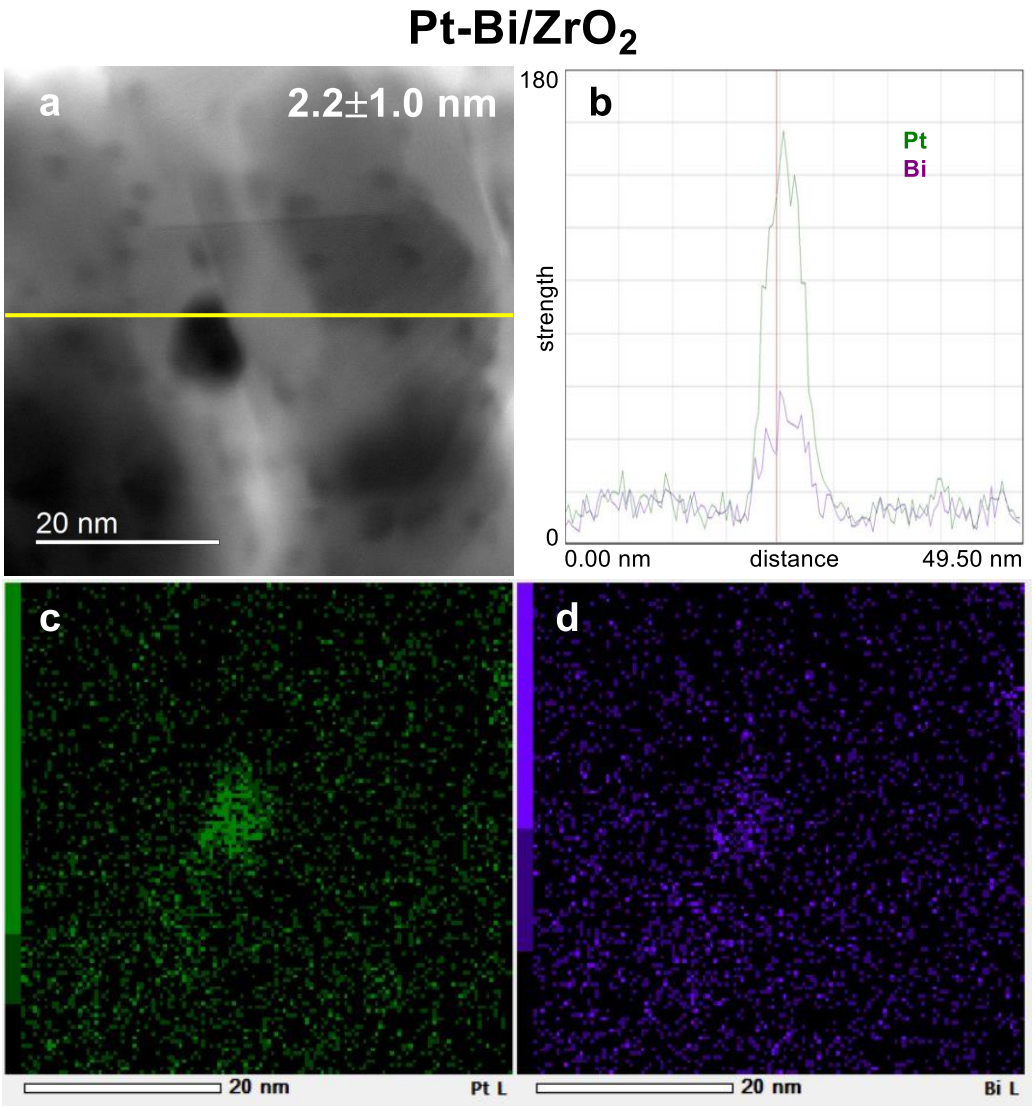

Figure 2. 5. BF-STEM and EDS images of Pt-Bi/ZrO_2 a) BF-STEM image b) EDS line analysis c) Pt EDS analysis d) Bi EDS analysis

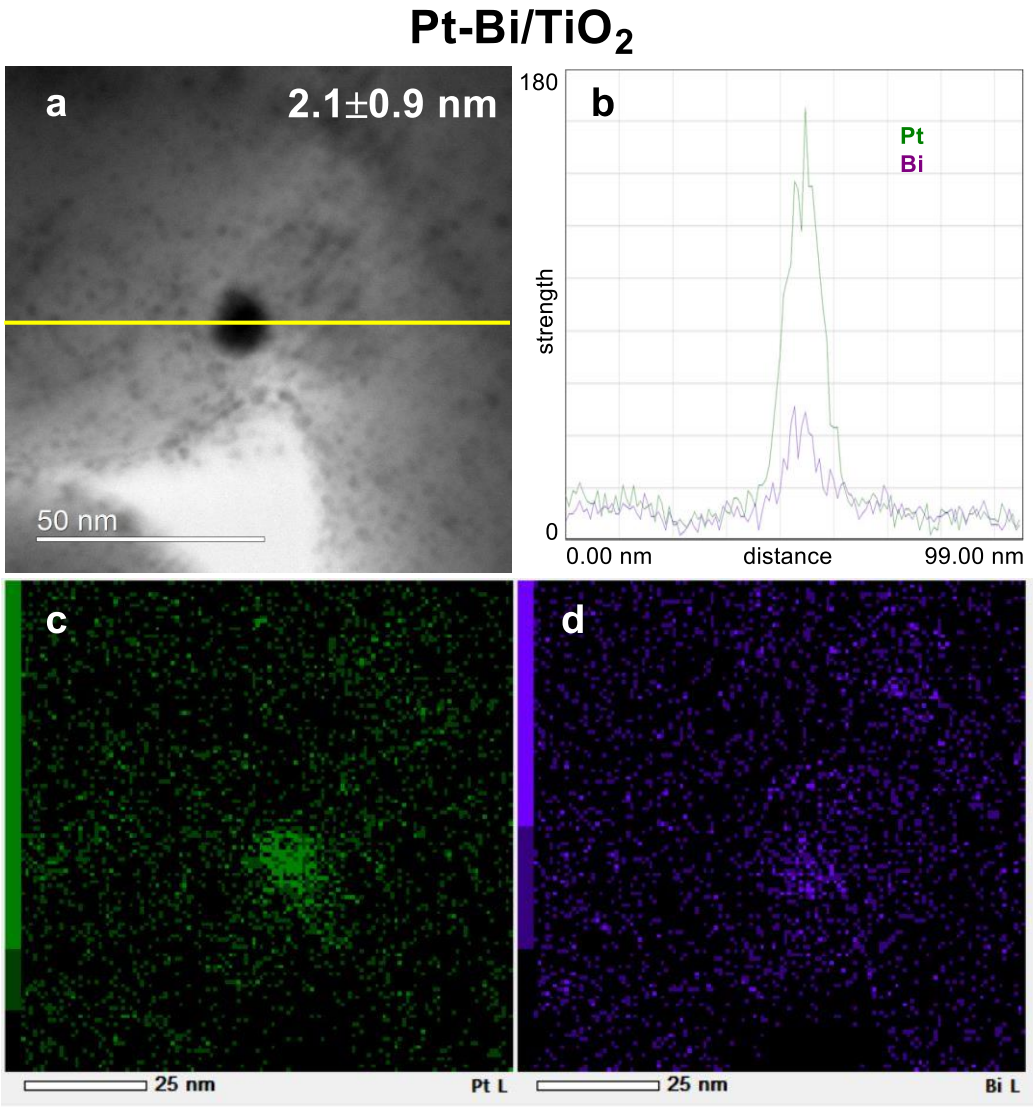

Figure 2. 6. BF-STEM and EDS images of Pt-Bi/TiO_2 a) BF-STEM image b) EDS line analysis c) Pt EDS analysis d) Bi EDS analysis

With the optimum catalyst in hand, the effect of the concentration of IPG aqueous solution in the oxidation was investigated. To compare the yield and selectivity of carboxylic acids for each support, oxidation of IPG was performed at several substrate concentrations with Pt-Bi/ZrO_2, Pt-Bi/TiO_2, or Pt-Bi/C catalyst (Figure 2.7). In the oxidation using Pt-Bi/C catalyst, the yield of HMB decreased as the concentration of IPG solution increased from 10 wt% to 20, 30, and 50 wt%, and the amount of acetal **4a** increased instead. In contrast, the highest HMB yields in the oxidation using Pt-Bi/ZrO_2 or Pt-Bi/TiO_2 catalysts (Pt-Bi/ZrO_2:77%, Pt-Bi/TiO_2:76%) were observed when the concentration of the IPG aqueous solution was 20 wt%. Additionally, the reactions with these catalysts in 30 wt% and 50 wt% concentration showed a higher yield of HMB and lower yields of acetal **4a** than the reactions

with the Pt-Bi/C catalyst in the same concentration. The higher the concentration of the reaction solution, the more acetal **4a** was produced. These results show that Pt-Bi/ZrO_2 and Pt-Bi/TiO_2 oxidize aldehyde **3a** to HMB faster than Pt-Bi/C, while the formation of acetal **4a** by Pt-Bi/ZrO_2 and Pt-Bi/TiO_2 is slower than that by Pt-Bi/C. This is assumed to be owing to the difference in polarity of the support surface, with the metal oxide support having a higher affinity for water and substrate than the activated carbon support. In contrast, the activated carbon support has a large volume due to its low bulk density and adsorbs the solution, causing the stirring efficiency is likely to decrease.

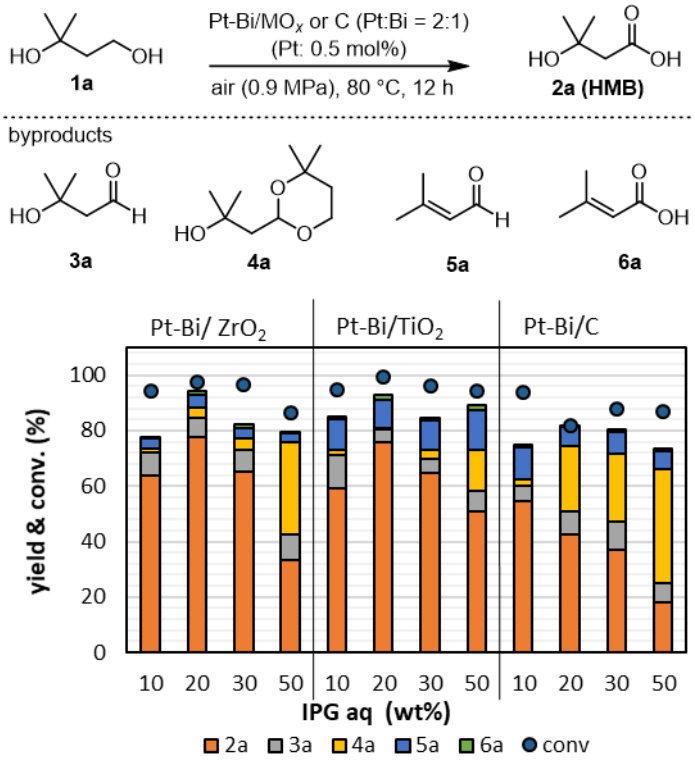

Figure 2. 7. Effect of IPG concentration for IPG oxidation in Pt-Bi/ZrO_2, Pt-Bi/TiO_2, and Pt-Bi/C catalysts. Pt-Bi catalyst: Pt-Bi/MO_x or C (Pt:Bi = 2:1)

To assess the recyclability of the Pt-Bi catalysts, we conducted recycle experiments (Figure 2.8). In the reactions with the Pt-Bi/C catalyst, the yield of HMB and the conversion of IPG had decreased as the number of catalyst reuses increased while the yield of acetal **4a** had increased. In contrast, in the reaction with Pt-Bi/ZrO_2 or Pt-Bi/TiO_2 catalyst, the yield of HMB had kept 60–80%, the conversion of IPG had kept over 90%, and the yield of acetal **4a** had not increased.

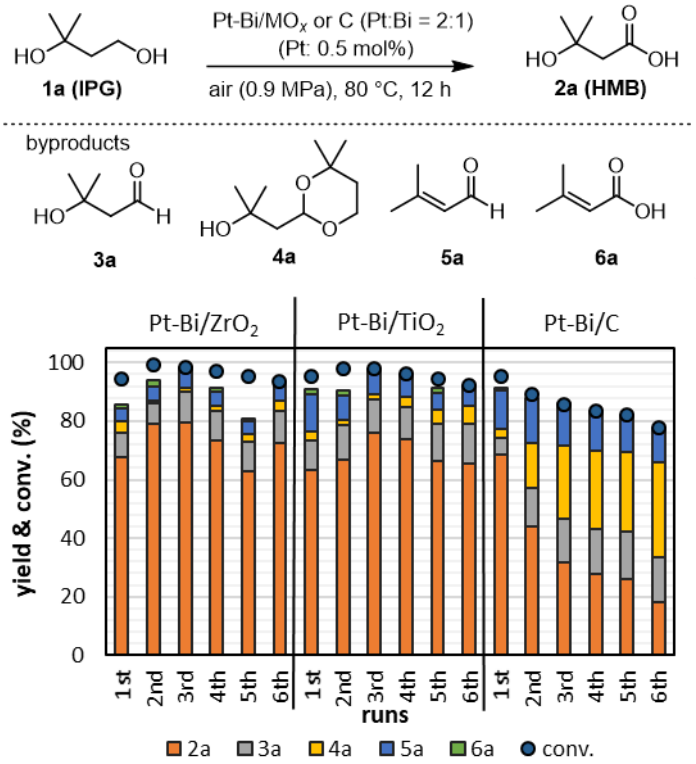

Figure 2. 8. Recycle experiments of Pt-Bi/ZrO_2, Pt-Bi/TiO_2 and Pt-Bi/C catalysts. Pt-Bi catalyst: Pt-Bi/MO_x or C (Pt:Bi = 2:1) 1a : 2.0 mmol (20 wt% aq)

To probe the origin of high recyclability of the Pt-Bi/ZrO_2 and TiO_2, we then investigated the particle sizes of the supported metal nanoparticles after the recycling experiments using BF-STEM images. In the fresh Pt-Bi/ZrO_2 and Pt-Bi/TiO_2 catalysts, the supported metal NPs were uniformly distributed with an average particle size of 2.2 and 2.1 nm, respectively while the average particle size of the fresh Pt-Bi/C catalyst was 1.4 nm, the value of which is smaller than that of the Pt-Bi/ZrO_2 and the Pt-Bi/TiO_2. Regarding the investigation of the used catalysts, analyses were performed after six-time reused samples, and cohesive metal particles were observed. The average particle sizes of the used Pt-Bi/MO_x catalysts in BF-STEM images were 6.8 ± 3.9 nm (Pt-Bi/ZrO_2), and 4.0 ± 2.0 nm (Pt-Bi/TiO_2). In contrast, the metal NPs of Pt-Bi/C showed a bimodal distribution with the average particle size of 3.2 ± 3.0 nm and 48.2 ± 14.1 nm for the small and large NPs, respectively. These results suggest that the high recyclability of the Pt-Bi/ZrO_2 and TiO_2 catalysts be attributable to the strong interactions between the metal NPs and metal oxide supports.

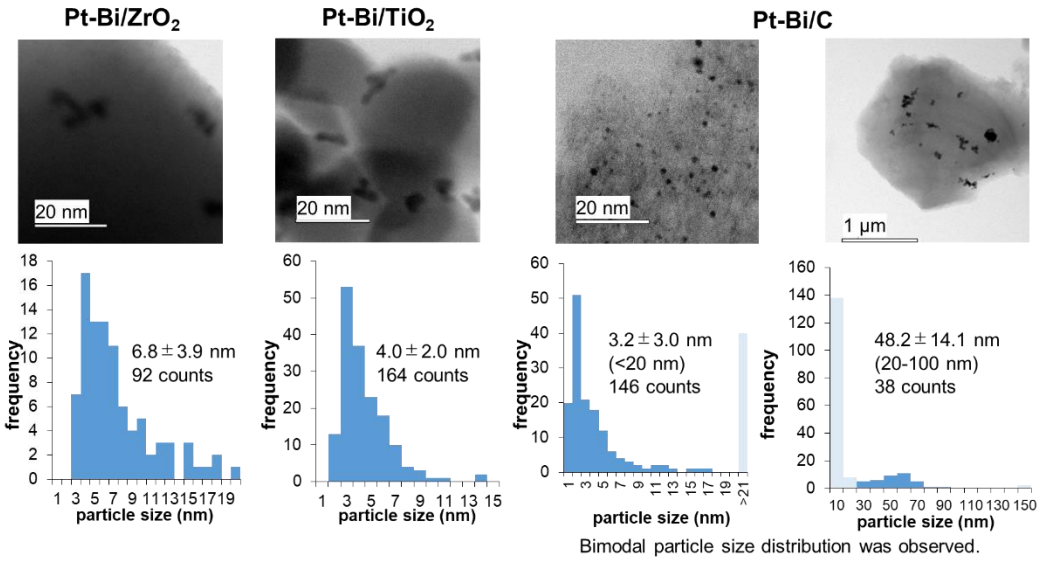

Figure 2. 9. BF-STEM images and average particle size of six times recycled Pt-Bi catalysts

To reveal the origin of the difference in the catalyst recyclability, we investigated the leaching of the Pt and Bi species on the Pt-Bi/ZrO_2, Pt-Bi/TiO_2, and Pt-Bi/C catalysts (Table 2.3). Both Pt and Bi species of Pt-Bi/ZrO_2 were not considerably decreased after the reaction. Concerning the Pt-Bi/TiO_2, little leaching of Pt species was observed while Bi species were lost by half after the reaction. In contrast to Pt-Bi catalysts supported on the metal oxides, Pt-Bi/C lost more than half of the Pt species as well as Bi species after the reaction. These results suggested that serious leaching of Pt and Bi species from Pt-Bi/C resulted in the decrease in catalytic activity observed in the recycling experiments (Figure 2.8). Because of the results, Pt-Bi/ZrO_2 was selected as the best catalyst.

Table 2. 3. Pt and Bi amount of fresh/used Pt-Bi/ZrO_2, Pt-Bi/TiO_2, and Pt-Bi/C catalysts

catalyst	Pt (wt%)		Bi (wt%)	
	fresh	**used**	**fresh**	**used**
Pt-Bi/ZrO_2	2.00	1.89	0.97	0.88
Pt-Bi/TiO_2	1.84	1.87	1.02	0.49
Pt-Bi/C	1.41	0.61	1.11	0.43

We then investigated the oxidation state of the Pt and Bi species of the fresh and six-time reused Pt-Bi/ZrO_2 catalysts with X-ray photoelectron spectroscopy (XPS) (Figure 2.9). Pt 4f spectra of the fresh Pt-Bi/ZrO_2 catalyst showed peaks at binding energies of 70.80 eV (Pt $4f_{7/2}$) and 74.10 eV (Pt $4f_{5/2}$), suggesting that Pt species of the catalyst were primarily in the Pt(0) state (Figure 6a). Additionally, peaks attributed to Pt(2+) (72.2 eV, Pt $4f_{7/2}$, 75.5 eV, Pt $4f_{5/2}$) and Pt(4+) (74.1 eV, Pt $4f_{7/2}$, 77.4 eV, Pt

$4f_{5/2}$) are also observed.[2.20] From the area ratio of these peaks, the molar ratio of Pt(0), Pt(+2), and Pt(+4) species on the fresh Pt-Bi/ZrO_2 catalyst was found to be 76:18:6. As for the XPS spectra of the recovered Pt-Bi/ZrO_2 catalyst after used six times, pairs of peaks assigned to the Pt(0), Pt(2+), and Pt(4+) species were observed at 70.6 eV (Pt $4f_{7/2}$) and 73.8 eV (Pt $4f_{5/2}$), 72.1 eV ($4f_{7/2}$) and 75.3 eV ($4f_{5/2}$), and 73.9 eV ($4f_{7/2}$) and 77.1 eV ($4f_{5/2}$), respectively. In comparison with the XPS spectra for the fresh Pt-Bi/ZrO_2 catalyst, Pt(0) area ratio was decreased by 6% and the area ratio of Pt(+2) and Pt(+4) was increased (Figure 6c). On the other hand, Bi 4f spectra of the fresh catalyst showed pairs of peaks at binding energies of 156.9 eV (Bi $4f_{7/2}$) and 162.2 eV (Bi $4f_{5/2}$), 159.1 eV (Bi $4f_{7/2}$) and 167.4 eV (Bi $4f_{5/2}$), which were attributable to Bi(0) and Bi(3+), respectively in a molar ratio of 39:61 (Figure 6b)[2.21]. Peaks of the Bi(0) and Bi(3+) species were also observed at the binding energies of 156.87 eV (Bi $4f_{7/2}$), 162.17 eV (Bi $4f_{5/2}$), 159.02 eV (Bi_2 $4f_{7/2}$), and 167.32 eV (Bi $4f_{5/2}$) for the Bi 4f spectra of the used Pt-Bi/ZrO_2. The molar ratio of Bi(0): Bi(3+) was changed from 39:61 to 17:83 (Figure 6d). Considering that Pt(2+) and Pt(4+) are unlikely to be active species in aerobic oxidation of alcohols[2.22], one of the roles of Bi species is presumably to suppress the deactivation of Pt(0) by having Bi(0) oxidized instead of Pt(0) [2.19][2.23]

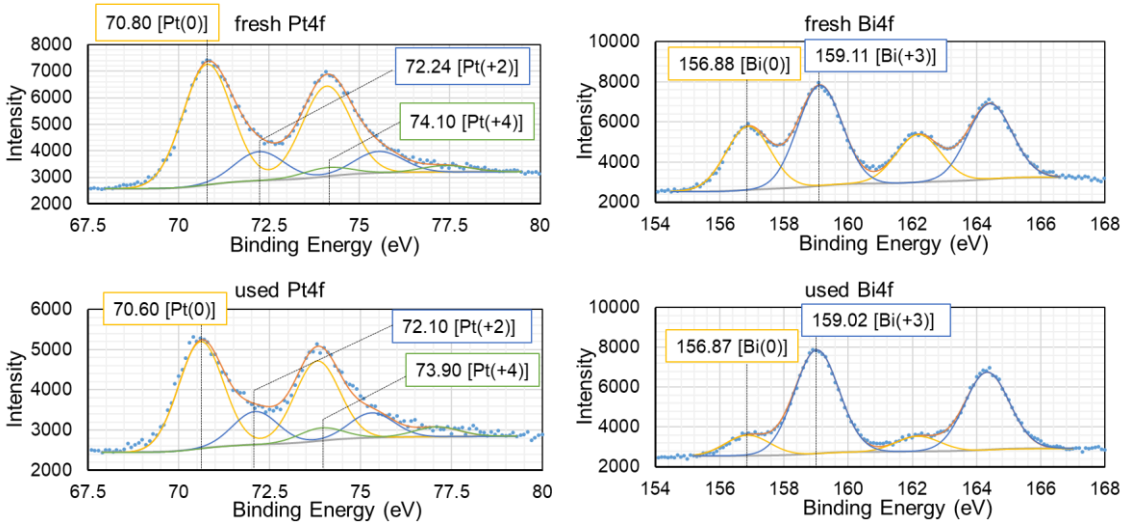

	Pt(0):Pt(+2):Pt(+4) [area%]	Bi(0):Bi(+3) [area%]
fresh	76:18:6	39:61
used	70:22:8	17:83

Figure 2. 10. XPS (X-ray Photoelectron Spectroscopy) spectra of fresh/used Pt-Bi/ZrO_2 catalyst. a) Pt4f XPS image of fresh catalyst, b) Bi4f XPS image of fresh catalyst, c) Pt4f XPS image of used catalyst, d) Bi4f XPS image of used catalyst

Conclusions

In summary, we reported that by using the Pt-Bi alloy catalysts using ZrO_2 or TiO_2 as support, HMB

(**2a**) can be obtained with a higher yield up to 77% and higher catalyst reusability than the catalyst of activated carbon support. The Pt-Bi/ZrO_2 and the Pt-Bi/TiO_2 catalysts exhibited less aggregation and leaching of Pt than the Pt-Bi/C catalyst in the oxidation. This difference may have brought higher yields of HMB and better catalyst recycling. The optimum concentration of the IPG aqueous solution is 20 wt%, and further raising this is a future task.

References

[2.1] J. Rathmacher, J. Fuller, Jr., S. Baier, S. Nissen and N. Abumrad, US patent appl. No. 16/903843.

[2.2] J. Peter, M. S. Fitschen, J. W. Gabriel, M. W. Jacob and R. W. Kenneth, *Nutrition*, 2013, **29**, 29–36.

[2.3] C. M. Prado, S. A. Purcell and A. Laviano, *J. Cachexia Sarcopenia Muscle*, 2020, **11**, 366–380.

[2.4] S. Nissen, R. Sharp, M. Ray, J. A. Rathmacher, D. Rice, J. C. Fuller Jr., A. S. Connelly and N. Abumrad, *J. Appl. Physiol.* 1996, **81**, 2095.

[2.5] T. Kurata, X. Xie and T. Shimada, Japan patent appl. No. 2019―181818.

[2.6] Y. E. Li, US patent appl. No. PCT/US2012/050893.

[2.7] N. Christian, S. Leo, R. Bruno, H. Paul and B. Anja, EP patent appl. No. PCT/EP2012/066154.

[2.8] M. Philippe, EP patent appl. No. PCT/EP2010/063460.

[2.9] (a) D. Shi, J. Liu and S. Ji, *Ind. Eng. Chem. Res.,* 2017, **56**, 11028–11033. (b) C.-R. Chang, X.-F. Yang, B. Long and J. Li, *ACS Catal.,* 2013, **3**, 1693–1699. (c) J. Liu, X.-M. Cao and P. Hu, *Phys. Chem. Chem. Phys.,* 2014, **16**, 4176–4185. (d) C. Shang and Z.-P. Liu, *J. Am. Chem. Soc.,* 2011, **133**, 9938–9947. (e) S. Biella, G.L. Castiglioni, C. Fumagalli, L. Prati and M. Rossi, *Catal. Today*, 2002, **72**, 43–49. (f) L. Prati and M. Rossi, *J. Catal.,* 1998, **176**, 552−560.

[2.10] (a) C. Zhou, Z. Guo, Y. Dai, X. Jia, H. Yu and Y. Yang, *Appl. Catal., B: Environ.,* 2016, **181**, 118–126. (b) S. E. Davis, M. S. Ide and R. J. Davis, *Green Chem.*, 2013, **15**, 17–45. (c) G. R. Summerhayes, M. Leavesley, A. Fairbairn, H. Mandui, J. Field, A. Ford and R. Fullagar, *Science,* 2010, **330**, 74–78. (d) D. D. Hibbitts and M. Neurock, *J. Catal,.* 2013, **299**, 261−271. (e) D. Mao, J. Qiu, M. Jia, X.- F. Zhang and J. Yao, *J. Phys. Chem. Solids,* 2019, **135**, 109095. (f) T. Mallat, Z. Bodnar, P. Hug and A. Baiker, *J. Catal.,* 1995, **153**, 131–143.

[2.11] (a) J. Xie, P. Duan, N. Kaylor, K. Yin, B. Huang, K. Schmidt-Rohr and R. J. Davis, *ACS Catal.,* 2017, **7**, 6745–6756. (b) S. Chibani, C. Michel, F. Delbecq, C. Pinelb and M. Besson, *Catal. Sci. Technol.* 2013, **3**, 339–350. (c) Y. H. Ng, S. Ikeda, T. Harada, Y. Morita and M. Matsumura, *Chem. Commun.,* 2008, 3181−3183. (d) M. S. Ide and R. J. Davis, *J. Catal.,* 2013 **308** 50–59. (e) M. S. Ide, D. D. Falcone and R. J. Davis, *J. Catal.,* 2014, **311**, 295–305. (f) J. Xie, B. Huang, K. Yin, H. N. Pham, R. R. Unocic, A. K. Datye and R. J. Davis, *ACS Catal.*, 2016, **6**, 4206–4217. (g) Y. Ryabenkova, P. J. Miedziak, D. W. Knight, S. H. Taylor and G. J. Hutchings, *Tetrahedron*, 2014, **70**, 6055–6058. (h) P. Fordham, M. Besson and P. Gallezot, *Catal. Lett.,* 1997, **46**, 195–199.

[2.12] For reviews, see; (a) M. Besson, P. Gallezot and C. Pinel, *Chem. Rev.,* 2014, **114**, 3, 1827–1870. (b) T. Mallat and A. Baiker, *Catal. Today,* 1994, **19**, 247–284. (c) M. Besson and P. Gallezot, *Catal. Today,* 2000, **57**, 127–141 (d) F. Liu, H. Wang, A. Sapi, H. Tatsumi, D. Zherebetskyy, H.-L. Han, L. M. Carl and G. A. Somorjai, *Catalysts,* 2018, **8**, 226.

[2.13] K. Mayahara and K. Oonishi, Japan patent appl. No. 1995―24689.

[2.14] Y. Nomura, Japan patent appl. No. PCT/JP2015/085175.

[2.15] (a) B. Jørgensen, S. E. Christiansen, M. L. D. Thomsen and C. H. Christensen, *J. Catal.*, 2007, 251, 332–337 (b) H. Tatsumi, F. Liu, H.-L. Han, L. M. Carl, A, Sapi and G. A. Somorjai, *J. Phys. Chem. C,* 2017, **121**, 7365–7371.

[2.16] (a) Y. Yamane, X. Liu, A. Hamasaki, T. Ishida, M. Haruta, T. Yokoyama and M. Tokunaga, *Org. Lett*., 2009, **11**, 5162–5165. (b) Z. Zhang, T. Hashiguchi, T. Ishida, A. Hamasaki, T. Honma, H. Ohashi, T. Yokoyama and M. Tokunaga, *Org. Chem. Front.*, 2015, **2**, 654–660. (c) Z. Zhang, Q. Wu, T. Hashiguchi, T. Ishida, H. Murayama and M. Tokunaga. *Catal. Commun.,* 2016, **87**, 1. (d) Z. Zhang, Y. Kumamoto, T. Hashiguchi, T. Mamba, H. Murayama, E. Yamamoto, T. Ishida, T. Honma and M. Tokunaga, *ChemSusChem*, 2017, **10**, 3482–3489, (e) T. Ishida, Z. Zhang, H. Murayama and M. Tokunaga, *J. Synth. Org. Chem., Jpn*., 2017, **75**, 1150–1161. (f) Z. Zhang, T. Mamba, E. Yamamoto, H. Murayama, T. Ishida, T. Honma, T. Fujitani and M. Tokunaga, *Appl. Catal., B*, 2019, **246**, 100–110. (g) Q.-A. Huang, A. Haruta, Y. Kumamoto, H. Murayama, E. Yamamoto, T. Honma, M. Okumura, H. Nobutou and M. Tokunaga, *Appl. Catal. B Environ.*, 2021, **296**, 120333.

[2.17] (a) S. J. Tauster, S. C. Fung and R. L. Garten, *J. Am. Chem. Soc.* 1978, **100**, 170–175. (b) S. J. Tauster, S. C. Fung, R. T. K. Baker and J. A. Horsley, *Science*, 1981, **211**, 1121–1125. For reviews on SMSI, see; (b) Q. Fu and T. Wagner, *Surf. Sci. Rep.* 2007, **62**, 431–498. (c) C.-J. Pan, M.-C. Tsai, W.-N. Su, J. Rick, N. G. Akalework, A. K. Agegnehu and S.-Y. Cheng, *J. Taiwan Inst. Chem. Eng.* 2017, **74**, 154–186.

[2.18] G.-Y. Yang, S. Shao, Y.-H. Ke, C.-L. Liu and H.-F. Ren, *RSC Adv.*, 2015, **5**, 37112–37118

[2.19] (a) M. Oana, R. Hoffmann, H. D. Abrña, F. J. Disalvo, *Surf. Sci.* 2005, **574**, 1–16. (b) S. Feng, J. Yi, H. Miura, N. Nakatani, M. Hada and T. Shishido, *ACS Catal.,* 2020, **10**, 6071–6083.

[2.20] X. Ren, J. Li, S. Wang, D. Zhang and Y. Wang, *J. Chem. Technol. Biotechnol.,* 2020, **95**, 1675–1682.

[2.21] F. Changa, Q. Xua, F. Wua, M. Jiaoa, B. Denga and X. Hub, *Mater. Sci. Semicond. Process.,* 2018, **80**, 1–8.

[2.22] H. Göksu, H. Burhan, S. D. Mustafov and F. Şen, *Sci. Rep.*, 2020, **10**, 5439.

[2.23] C. Keresszegi, T. Mallat, J.-D. Grunwaldt and A. Baiker. *J. Catal.,* 2004, **225**, 138–146

Chapter 3. Unsymmetric Disulfane Synthesis by Thiol-Disulfane Exchange Reaction with Basic Zeolite

Abstract

The author reported the exchange reaction of thiol and one of the alkyl or arylsulfonyl groups of disulfane with Na-exchanged X type zeolite (Na-X), commercially available as MS-13X. This reaction proceeds at room temperature under air. Various functionalized thiols and disulfanes are tolerant in this reaction condition. Sterically-hindered disulfanes or electron-deficient thiol substrates also can be used; however, they require high temperatures under inert atmospheres to maintain good product yields. This reaction emitted only another thiol as a side product, which can be recycled as a substrate.

Introduction

The S-S bond is found in many natural products, and some of them are bioactive substances such as flavor in foods and pharmaceuticals [3.1].

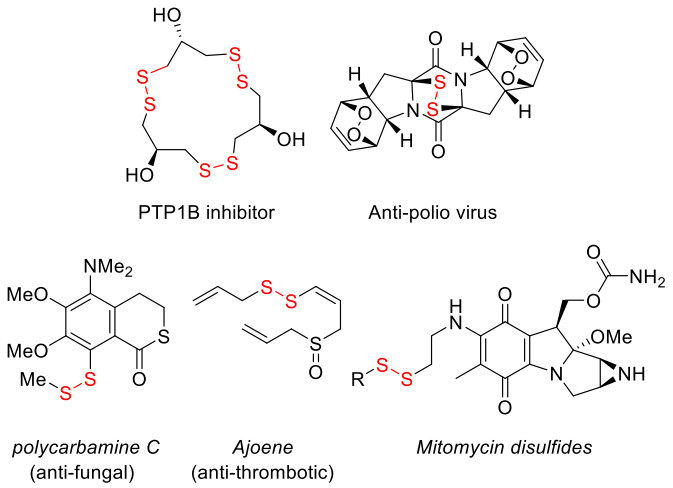

Figure 3. 1. Unsymmetrical disulfanes found in natural products and biologically active compounds

Many practical reactions to synthesize symmetrical disulfanes have been reported. However, few reactions to synthesize unsymmetrical disulfane were reported and these reports are not atom-economic or proceed on the limited substrate. S_N2 reductive reaction of thiol and sulfide compound which has to leave group on S atom used as a conventional method for synthesis of unsymmetrical disulfanes (Scheme 3.1A)[3.2]. The reaction needs a stoichiometric base and is required to prepare a sulfenylated derivative in a multi-step reaction. Oxidative S-S bond formation of different thiols, which is able to synthesize disulfane from two thiols directly, was also conventional. However, stoichiometric oxidant was needed and two types of thiols with different electronic states are required to avoid the generation of symmetrical disulfanes as a byproduct (Scheme 3.1B)[3.3]. Previous thiol-

disulfane exchange reaction is restricted to the structure of the leaving group and twice reactions are needed to synthesize desired unsymmetrical disulfanes (Scheme 3.1C)[3.4]. One step thiol-disulfane exchange reaction with KOH catalyst was reported. However, this reaction needs reflux condition and succeeded only 3 examples (Scheme 3.1D)[3.5].

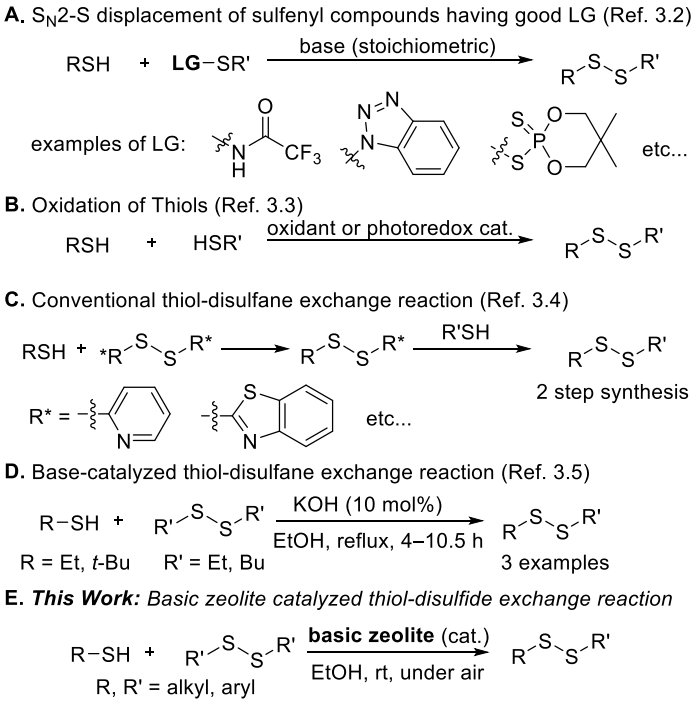

Scheme 3. 1. Synthetic methods of unsymmetrical disulfanes

To overcome these shortcomings, the author's group reported thiol-disulfane exchange reaction with Na-exchanged X type zeolite (Na-X)(Scheme 3.1E). This reaction produced the desired disulfane only one step at room temperature under air. Catalyst Na-X was reusable 10 times without decreasing the yield. The emitted thiol as a side product can be converted to symmetric disulfane by oxidative dimerization. Furthermore, this reaction has been confirmed to have a very wide substrate application range for both thiols and disulfanes. Herein, the author investigated additional optimization of reaction conditions and synthetic application.

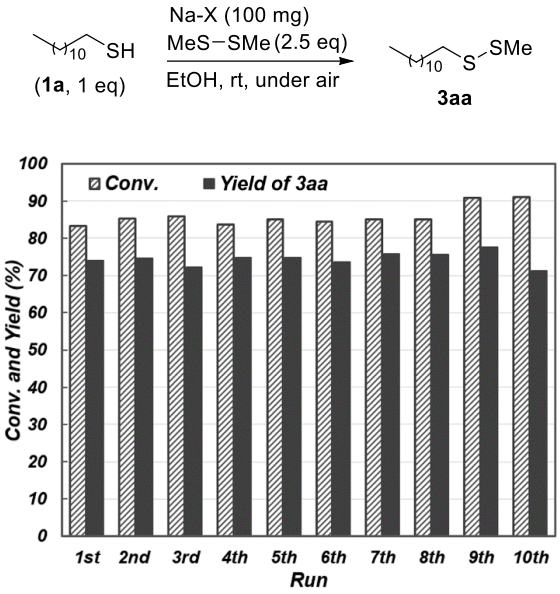

Figure 3. 2. Recyclability of the Na-X zeolite catalyst

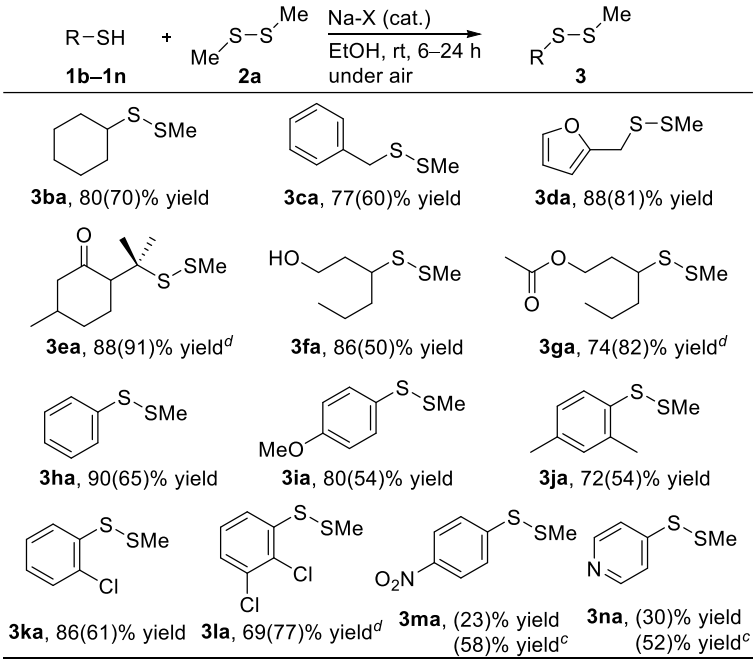

[a]A mixture of Na-X (100 mg), DMDS (3.0 mmol), thiol (1.0 mmol) in EtOH (2.0 mL) were stirred at rt under air for 6 – 24 h. Yield was analyzed by GC. Isolated yield was presented in parentheses. [b]DMDS: 2.0 equiv. [c]Reaction Conditions: 120 °C under N_2 for 24 h. [d]Isolated yields were higher than GC yields, which is attributable to the oxidative work-up process.

Scheme 3. 2. Substrate scope of thiols

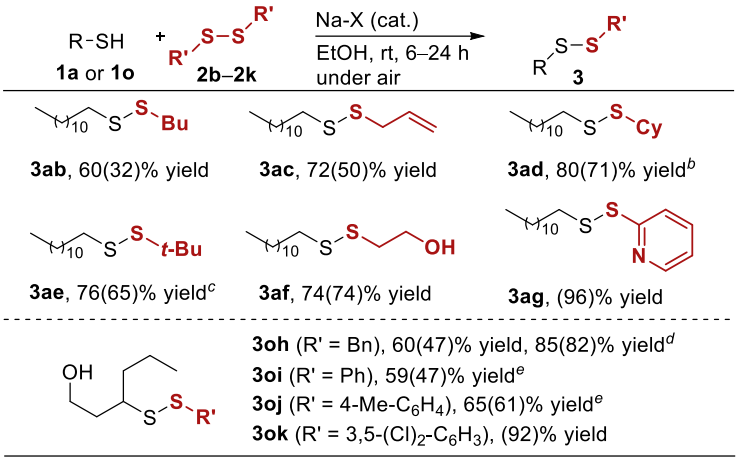

[a]Reaction Conditions: A mixture of Na-X (100 mg), disulfane (3,0 mmol), thiol (1.0 mmol) in EtOH (2.0 mL) were stirred at rt under air for 6–24 h. Yield was analyzed by GC. Isolated yield was presented in parentheses. [b]100 ºC under N_2. [c]150 ºC under N_2 for 72 h. [d]50 ºC. [e]Disulfane: 2.0 equiv.

Scheme 3. 3. Substrate scope of disulfanes and thiols[a]

Results and Discussions

Initially, the author explored the conditions of the thiol-disulfane exchange reaction of 1-dodecanethiol (**1a**) and (methyldisulfanyl)methane (DMDS, **2a**) (Table 3.1). In the PrOH solvent condition, conversion of **1a** was 98% and the yield of target compound **3aa** was 85% (entry 1). Without zeolite, Na-X condition showed a very low conversion of **1a** and yield of **3aa** (entry 2). Decreasing the reaction temperature to 10 ˚C slightly reduced the amount of byproduct **4a** (entry 3). The previous reaction using EtOH as solvent showed an 87% yield of **3aa** (entry 4). Therefore, EtOH is the most suitable solvent for this reaction. Using Amberlyst A26 (OH), which is a resin containing ammonium, as catalyst showed low selectivity of **3aa** compared with the reaction using zeolite Na-X (entry 5).

Table 3. 1. Optimization of reaction conditions [a]

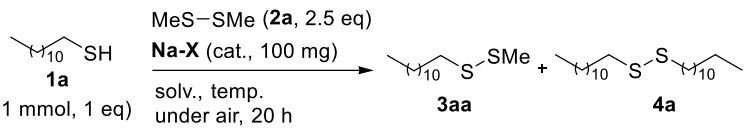

entry	catalyst	solvent	temp. [ºC]	**1a** conv. [%]	yield [%]	
					3aa	**4a**
1	Na-X	PrOH	rt	98	85	14
2	none	PrOH	rt	7	6	trace
3	Na-X	PrOH	10	98	85	12
4	Na-X	EtOH	10	90	87	3
5	Amberlyst A26 (OH)	EtOH	10	99	45	50
6	Na-X	MeOH	10	85	69	24
7	Na-X	CH_2Cl_2	10	5	<1	<1
8	Na-X	THF	10	6	<1	<1
9	Na-X	Toluene	10	4	<1	2
10	Na-X	DMF	10	94	10	84
11	NH_4-X	EtOH	10	35	30	6
12	K-A	EtOH	10	90	71	14
13	Na-A	EtOH	10	89	70	14
14	Ca/Na-A	EtOH	10	30	28	2
15[b]	Et_3N	EtOH	10	90	75	7
16[b]	K(O-*t*-Bu)	EtOH	10	96	5	92
17[c]	Na-X	EtOH	10	97	94	4

Entries 1-5: This work, Entries 6-17: Previous report, [a] Reaction conditions: A mixture of catalyst (100 mg), disulfane **2a** (2.5 mmol), thiol **1a** (1.0 mmol) in a solvent (2.0 mmol) were stirred under air for 20 h. The yields were determined by GC. Na-X: MS-13X, K-A: MS3A, Na-A: MS4A, Ca/Na-X: MS5A, [b] 5 mol.% of catalyst was used, [c] DMDS (10 eq.) was used.

To the extent the thiol-disulfide exchange to a practical reaction, the author performed gram scale reaction and chiral substrate reaction (Scheme 3.4). In the former reaction, 10.1 g of **1a** and 5 equivalent of **2a** were mixed under reaction conditions then **3aa** was obtained in 81% isolated yield (Scheme 3-4a). In the latter part, N-Boc-(*R*)-cysteine ((*R*)-**1p**) (>99%ee) was reacted two species of symmetric disulfane **2a** and **2c**. These reactions produced 86% (**3pa**) and 85% (**3pc**) yield of unsymmetrical disulfane without decreasing of enantiomeric excess (Scheme 3-4b).

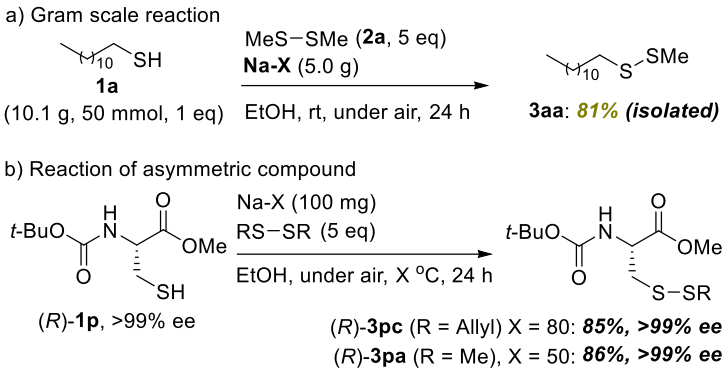

Scheme 3. 4. Synthetic application

Conclusions

In conclusion, the author reconfirmed that the reaction conditions were appropriate. The method turned out to be useful for gram-scale reactions and reactions with a chiral substrate. Further extension of the scope and synthetic application is currently underway in our laboratory.

General Procedures

Catalyst preparation

MS-13X was pulverized by a bowl mill. Pulverized zeolite (10 g) was stirred in 100 mL of 1.0 M aqueous solutions of NaCl at 80 ºC for 4 h. The resulting suspension was filtered, and the same cation exchange process was repeated three times. After that, the resultant solid was rinsed with deionized H_2O. Next, the zeolite was dried overnight at 100 ºC in drying and passed through a sifter (< 125 μm). The water content of Na-X was 24% of the total weight.

Reaction procedures

General procedures for thiol–disulfane exchange reaction: Na-X [100 mg including moisture (24 wt% of H_2O)], DMDS (235.5 mg, 2.5 mmol), EtOH (2.0 mL), and a stirring bar were placed in a 10 mL screw vial. 1-Dodecanethiol (202.4 mg, 1.0 mmol) was added to the vial, and the solution was stirred at 10 ºC for 20 h. Diglyme (32.8 mg, 0.24 mmol) was added to the mixture as internal standard. The resulting mixture was centrifuged and filtered to remove the Na-X catalyst and analyzed the yield and conversion by GC.

Procedures for using PrOH as solvent at room temperature: Na-X [100 mg including moisture (24 wt% of H_2O)], DMDS (235.5 mg, 2.5 mmol), PrOH (2.0 mL), and a stirring bar were placed in a 10 mL screw vial. 1-Dodecanethiol (202.4 mg, 1.0 mmol) was added to the vial, and the solution was stirred at room temperature for 20 h. Diglyme (32.8 mg, 0.24 mmol) was added to the mixture as internal standard. The resulting mixture was centrifuged and filtered to remove the Na-X catalyst and analyzed the yield and conversion by GC.

Procedures for using PrOH as solvent: Na-X [100 mg including moisture (24 wt% of H_2O)], DMDS (235.5 mg, 2.5 mmol), PrOH (2.0 mL), and a stirring bar were placed in a 10 mL screw vial. 1-Dodecanethiol (202.4 mg, 1.0 mmol) was added to the vial, and the solution was stirred at 10 ºC for 20 h. Diglyme (32.8 mg, 0.24 mmol) was added to the mixture as internal standard. The resulting mixture was centrifuged and filtered to remove the Na-X catalyst and analyzed the yield and conversion by GC.

Procedures for using Amberlyst A26 (OH) as a catalyst: Amberlyst A26 (OH) (100 mg), DMDS (235.5 mg, 2.5 mmol), EtOH (2.0 mL), and a stirring bar were placed in a 10 mL screw vial. 1-Dodecanethiol (202.4 mg, 1.0 mmol) was added to the vial, and the solution was stirred at 10 ºC for 20 h. Diglyme (65.6 mg, 0.49 mmol) was added to the mixture as internal standard. The resulting mixture was centrifuged and filtered to remove the resin catalyst and analyzed the yield and conversion by GC.

Procedures for gram scale reaction: Na-X (5.0 g), DMDS (117.7 mg, 1.25 mol), EtOH (100 mL), and a stirring bar were placed in a 500 mL flask. 1-Dodecanethiol (50.6 g, 250 mmol) was added to the vial, and the solution was stirred at 10 ºC for 20 h. Diglyme (8.2 g, 61.1 mmol) was added to the mixture as internal standard. The resulting mixture was filtered to remove the Na-X catalyst and analyzed the yield and conversion by GC. The filtrate was concentrated to remove EtOH and MeSH then diluted to isolate **3aa**.

Procedures for synthesis **3pa**: Na-X [100 mg including moisture (24 wt% of H_2O)], DMDS (0.471 g, 5.0 mmol), EtOH (2.0 mL), and a stirring bar were placed in a 10 mL screw vial. N-Boc-(*R*)-cysteine (>99%ee) (235.3 mg, 1.0 mmol) was added to the vial, and the solution was stirred at 50 ºC for 20 h. The resulting mixture was centrifuged and filtered to remove the Na-X catalyst. The filtrate was concentrated and purified by column chromatography.

Procedures for synthesis **3pc**: Na-X [100 mg including moisture (24 wt% of H_2O)], Diallyldisulfide (0.731 g, 5.0 mmol), EtOH (2.0 mL), and a stirring bar were placed in a 10 mL screw vial. N-Boc-(*R*)-cysteine (>99%ee) (235.3 mg, 1.0 mmol) was added to the vial, and the solution was stirred at 80 ºC for 20 h. The resulting mixture was centrifuged and filtered to remove the Na-X catalyst. The filtrate was concentrated and purified by column chromatography.

Reference

[3.1] C.-S. Jiang, W. E. G. Müller, H. C. Schröder, Y.-W. Guo, Chem. Rev. 2012, 112, 2179– 2207.

[3.2] a) R. Hunter, M. Caira, N. Stellenboom, J. Org. Chem. 2006, 71, 8268– 8271. b) M. Bao, M. Shimizu, Tetrahedron 2003, 59, 9655– 9659. c) J. Xue, X. Jiang, Nat. Commun. 2020, 11, 4170.

[3.3] a) J. K. Vandavasi, W.-P. Hu, C.-Y. Chen, J.-J. Wang, Tetrahedron 2011, 67, 8895– 8901. b) P. Huang, P. Wang, S. Tang, Z. Fu, A. Lei, Angew. Chem. Int. Ed. 2018, 57, 8115– 8119. c) J. Yuan, C. Liu, A. Lei, Org. Chem. Front. 2015, 2, 677– 680, d) D. H. Dethe, A. Srivastava, B. D. Dherange, B. V. Kumar, Adv. Synth. Catal. 2018, 360, 3020– 3025. e) R. Smith, X. Zeng, H. Müller-Bunz, X. Zhu,

Tetrahedron Lett. 2013, 54, 5348– 5350.

[3.4] a) E. Brzezinska, A. L. Ternay, Jr. J. Org. Chem. 1994, 59, 8239– 8244. b) C. Diaz, K. Balasubramanian, A. J. Schroit, Bioconjugate Chem. 1998, 9, 250– 254. c) D. Crich, V. Krishnamurthy, F. Brebion, M. Karatholuvhu, V. Subramanian, T. K. Hutton, J. Am. Chem. Soc. 2007, 129, 10282– 10294.

[3.5] D. T. McAllan, T. V. Cullum, R. A. Dean, F. A. Fidler, J. Am. Chem. Soc. 1951, 73, 3627– 3632.

[3.6] a) R. Singh, G. M. Whitesides, J. Am. Chem. Soc. 1990, 112, 1190– 1197. b) R. D. Bach, O. Dmitrenko, C. Thorpe, J. Org. Chem. 2008, 73, 12– 21. c) A. J. Parker, N. Kharasch, Chem. Rev. 1959, 59, 583– 628. d) R. Singh, G. M. Whitesides, in Supplement S The Chemistry of Sulphur-Containing Functional Groups (Eds.: S. Patai, Z. Rappoport), John Wiley & Sons, Chichester, 1993, pp. 633– 658.

Chapter 4. H_2S Free Synthesis of Polysulfane with Heterogenous Cobalt Catalyst

Abstract

The author explored a new synthesis method of polysulfane without H_2S gas. The author investigated conditions of catalyst, H_2 gas pressure, S_8 equivalent, and reaction temperature. As a result, the author expects to analyze the yield of polysulfane in detail.

Introduction

Polysulfanes reduce friction during the processing of metal products by being added to lubricants. Therefore, the demand is increasing in the field of tribology [4.1]. Polysulfanes are synthesized from alkenes, sulfur, and H_2S using amines as catalysts (Scheme 4.1a) [4.2]. However, since H_2S is toxic and difficult to handle, a synthesis method of polysulfanes without H_2S has been required. Emmanuel and Yoneda reported polysulfane synthesis method from thiol and sulfur (Scheme 4.1b) [4.3]. In this method, polysulfanes are synthesized without H_2S, although H_2S is eventually required for the synthesis of thiols.

On the other hand, the author's group has reported that polysulfanes were obtained in 88% conversion when alkenes were mixed with sulfur in butanol under a hydrogen atmosphere (Scheme 4.2a) [4.4a]. In addition, the reaction was proceeded without solvent by Co_3O_4 and zeolite Na-X (Scheme 4.2b) [4.4b]. However, this method also obtained thiols. The author developed the H_2S free polysulfane synthesis in this study.

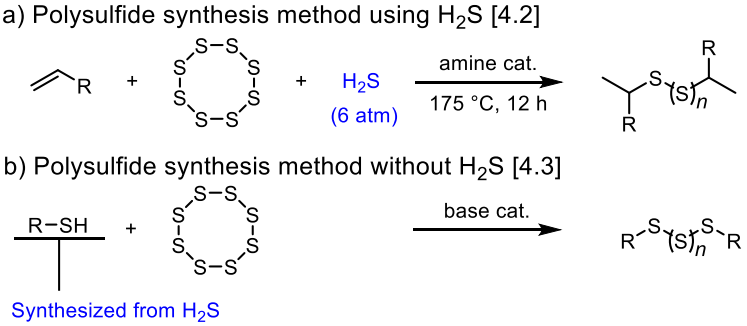

Scheme 4. 1. Previous Method of Polysulfane Synthesis.

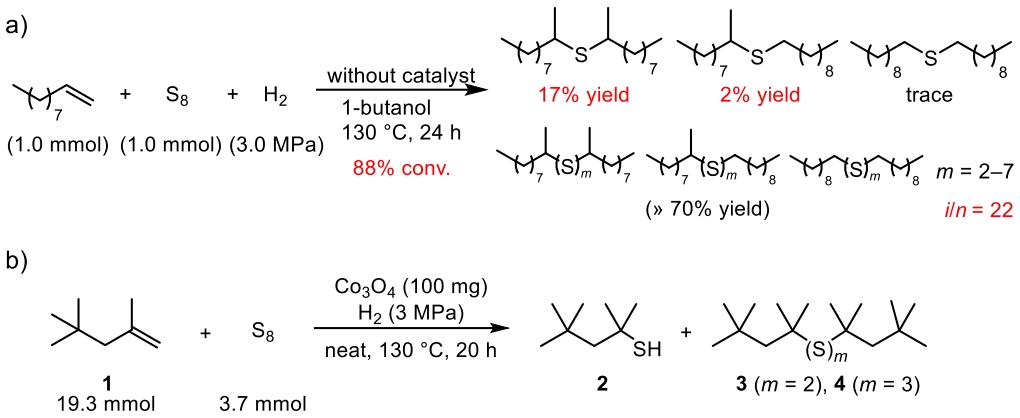

entry	additive	conv. (**1**, mmol)	yield[a] (**2**, mmol)	yield[a] (**3**, mmol)	yield[a] (**4**, mmol)
1	none	11.0	8.43	0	0
2	Na-X (100 mg)	14.6	6.10	0.61	3.85

Reaction was carried out in a stainless steel autoclave.

a) Yields and conversion were determined by GC.

Scheme 4. 2. Studies of polysulfane synthesis of our group [4.4]

General Procedures

General procedures for the synthesis of cobalt sulfide [4.5]: Cobalt acetate tetrahydride [$Co(OAc)_2{\cdot}4H_2O$ (2.2 g, 8.8 mmol)], sulfur [S_8 (0.57 g, 2.2 mmol)], H_2O (114 mL) and hydrazine monohydride [$H_2NNH_2{\cdot}H_2O$ (11 mL)] were put into 200 mL autoclave. Air in the autoclave was replaced with N_2 gas. The autoclave was stirred at 600 rpm and heated in 2 ºC/min then stirred at 180 ºC for 22 h. The resultant mixture was cooled to room temperature followed by removing the water layer by filtration and washing collected black powder with H_2O, EtOH, and Et_2O.

General procedures for polysulfane synthesis: Cobalt sulfide, Na-X zeolite, and S_8 were put into 40 mL autoclave. Isobutenedimer (20 mmol) was added to the mixture. Air in the autoclave was replaced with H_2 gas. The autoclave was heated and stirred at 800 rpm. After the reaction, the autoclave was cooled at 0 ºC, then tridecane (2.0 mmol) was added as internal standard. The resulted mixture was centrifuged and filtrated to remove the catalyst. A little amount of the supernatant was picked and diluted with hexane. The sample was analyzed by GC.

Results and Discussions

Initially, metal oxide catalyst was explored. Oxide of cobalt, molybdenum, nickel, and copper were used as catalysts for the synthesis of polysulfane (Table 4.1). As the result, cobalt oxides was the best in these metal oxide (entries 1-4). Additionally, since the cobalt oxide was converted to cobalt sulfide after the reaction, cobalt sulfide was used as a catalyst. The reaction produced a 77% yield of thiol and

a 0% yield of polysulfanes (entry 5).

Table 4. 1. Scope of catalyst species

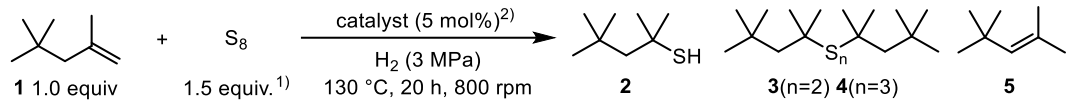

1 1.0 equiv + S_8 1.5 equiv.1) 130 °C, 20 h, 800 rpm → **2**, **3**(n=2) **4**(n=3), **5**

1) S atom standard, 2) metal atom standard

entry	catalyst	conv. (%)	yield [% (mmol)]				(%)
			2	**3**	**4**	**5**	**2+3+4**
1	Co_3O_4	70	2 (0.5)	1 (0.5)	9 (0.9)	6 (1.2)	12
2	MoO_3	53	0 (0.0)	0 (0.0)	1 (0.1)	16 (3.2)	2
3	NiO	51	0 (0.0)	<1 (<0.1)	3 (0.3)	3 (0.7)	3
4	CuO	41	0 (0.0)	0 (0.0)	1 (0.1)	4 (0.7)	1
5	Co_3S_4	85	77 (15.2)	0 (0.0)	0 (0.0)	5 (1.1)	77

Over cleavage of S–S bond was presumed to result in generating of thiol, then the effect of catalyst equivalent was investigated (Table 4.2). Decreasing cobalt sulfide to 2.5 mol% gave 85% yield of thiol **2** and 7% yield of disulfane **3** (entry 2). More decreasing to 0.5 mol% showed a very little yield of thiol **2** (<1%); however, the yield of polysulfanes was only 1% (disulfane **3**) and 10% (trisulfane **4**) (entry 3). Zeolite Na-X, which proceeds S-S bond exchange, was added to improve the yield of polysulfane (entries 4-5). The yields were up to 2% (**3**) and 21% (**4**) (entry 5).

Table 4. 2. Scope of catalyst and additive

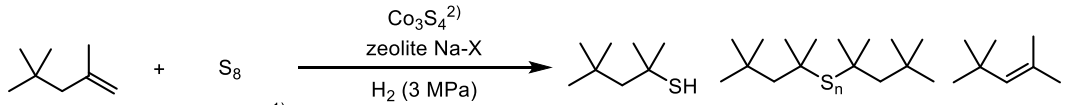

1 1.0 equiv. + S_8 1.5 equiv.1) 130 °C, 20 h, 800 rpm → **2**, **3**(n=2) **4**(n=3), **5**

1) S atom standard, 2) metal atom standard

entry	Co_3S_4 (mol%)	Na-X (mg)	conv. (%)	yield [% (mmol)]				(%)
				2	**3**	**4**	**5**	**2+3+4**
1	5.0	0	85	77 (15.2)	0 (0.0)	0 (0.0)	5 (1.1)	77
2	2.5	0	85	80 (15.9)	7 (0.7)	0 (0.0)	5 (1.1)	87
3	0.5	0	76	<1 (0.2)	1 (0.1)	10 (1.0)	7 (1.3)	11
4	0.5	10	78	4 (0.7)	2 (0.2)	14 (1.4)	7 (1.4)	19
5	0.5	100	87	5 (1.0)	2 (0.2)	21 (2.1)	4 (0.8)	28

To improve the yield of polysulfanes, H_2 gas pressure and the equivalent of S_8 were explored (Table 4.3). Raising H_2 pressure to 5 MPa to generate more HS_nH species and improve the yield of

polysulfans resulted in only increasing the yield of thiol **2** (entry 2). This is because only S-S bond cleavage proceeded and the reaction of alkene **1** and HS_nH species was not activated. In exploring the equivalent of sulfur, 3.0 equivalent of S_8 resulted in inhibiting the generation of thiol. However, the yield of disulfane **3** and trisulfane **4** also decreased (**3**: 1%, **4**: 12%) (entry 3). More cobalt sulfide was added then the yields of **3** and **4** were recovered (entry 4).

Table 4. 3. Equivalent of substrate

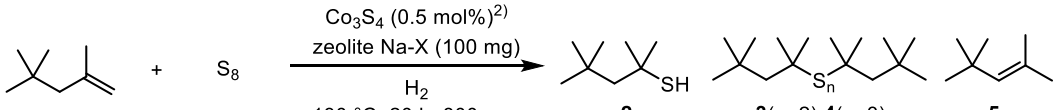

1 1.0 equiv. **2** **3**(n=2) **4**(n=3) **5**

1) S atom standard, 2) metal atom standard, 3) Co_3S_4 2.5 mol%

entry	S_8 (equiv.)[1)]	H_2 (MPa)	conv. (%)	yield [% (mmol)] **2**	**3**	**4**	**5**	(%) **2+3+4**
1	1.5	3	87	5 (1.0)	2 (0.2)	21 (2.1)	4 (0.8)	28
2	1.5	5	84	19 (3.7)	2 (0.2)	22 (2.2)	5 (1.1)	43
3	3.0	3	94	<1 (0.2)	1 (0.1)	12 (1.2)	2 (0.5)	15
4[3)]	3.0	3	98	8 (1.7)	2 (0.2)	23 (2.2)	<1 (0.2)	33

The author investigated the reaction temperature (Table 4.5). The yields at 120 ºC were 49% (2), 6% (3) and 44% (4) (entry 2). However, the yields at 115 ºC decreased to 16% (2), 2% (3), and 25% (4) (entry 3). In contrast, increasing to 150 ºC showed an increasing rate of 2,3, and 4 (entries 4 and 5).

Table 4. 4. Scope of reaction temperature

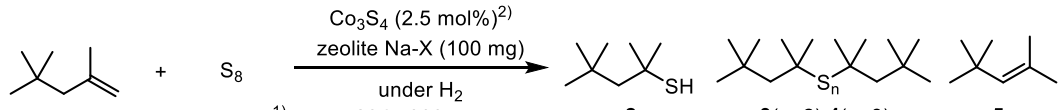

1 1.0 equiv. 2.0 equiv[1)] **2** **3**(n=2) **4**(n=3) **5**

1) S atom standard, 2) metal atom standard

entry	H_2 (MPa)	temp (ºC)	conv. (%)	yield [% (mmol)] **2**	**3**	**4**	**5**	(%) **2+3+4**
1	3	130	91	56 (11.1)	6 (0.6)	30 (3.0)	3 (0.6)	92
2	3	120	94	49 (9.7)	6 (0.6)	44 (4.4)	2 (0.4)	99
3	3	115	91	16 (3.2)	2 (0.2)	25 (2.5)	3 (0.7)	43
4	2	130	89	3 (0.7)	2 (0.2)	21 (2.1)	4 (0.9)	27
5	2	150	88	13 (2.5)	12 (0.2)	26 (2.6)	4 (0.9)	51
6	2	120	95	14 (2.7)	3 (0.3)	38 (3.8)	2 (0.4)	55

Conclusions

In conclusion, H_2S free polysulfane synthesis has several improvements. This reaction is proceeded by using cobalt sulfide instead of cobalt oxide and adding zeolite Na-X. However, excess cobalt sulfide, H_2 pressure, and S_8 result in decreasing polysulfanes yield. The most appropriate reaction temperature depends on other conditions. Since the conversion rates of the substrates and the yields of the products are very different in all the results in this study, the author needs to analyze n>4 polysulfanes generated in this reaction.

References

[4.1] a) W. Hua, L. Jing, Y. Hongling, Z. Xiangqiong, L. Lingbo, R. Tianhui, *Tribol. Int.*, 2007, 40, 1246–1252, b) J. Li, H. Ma, T. Ren, Y. Zhao, L. Zheng, C. Ma, Y. Han, Appl. Surf. Sci. 2008, 254, 7232-7236, c) Y. Hongling, D. Kunyang, Z. Xiangqiong, S. Heyang, R. Tianhui, *Industrial Lubrication and Tribology; Bradford*, 2008, 60, 79–85. d) F. Xisheng, S. Heyang, R. Tianhui, L. Weimin, X. Qunji. *Industrial Lubrication and Tribology; Bradford*, 2006, 58, 145–150. e) J. Li, H. Wu, T. Ren, *J. Tribol.* 2009, 131, 011801 f) H. Y. Shao, Y. M. Liu, X. S. Fu, T. H. Ren, *J. Synth. Lubr.* 2005, 22, 259–270. g) M. Miyajima, K. Kitamura, K. Matsumoto, *Tribology Online*, 2015, 10, 225–231.

[4.2] a) E.W. Qian, S. Yamada, J. Lee, S. Otsuki, M. Ishii, D. Ota, K. Hirabayashi, A. Ishihara, T. Kabe, *Appl. Catal. A: Gen.* 2003, 253, 15–27. b) K. Ibi, S. Yamada, patent application N.O. JP2001-186434 (2001).

[4.3] a) Y. Yoneda, H. Sakata, patent application N.O. PCT/JP2016/08184, WO 2017/104273 (2016). b) A. Emmanuel, Eur. Pat. Appl. 1989/EP89400842A (1989)

[4.4] a) M. Kimura, master's thesis of Kyushu university, 2019. b) K. Takakura, master's thesis of Kyushu university, 2020.

[4.5] I. Sorribes and A. Corma, *Chem. Sci.*, 2019, **10**, 3130–3142

Acknowledgments

I would like to express my sincere gratitude to Professor Makoto Tokunaga for accepting me as a member of the laboratory and always warmly encouraging me. I also appreciate assistant professor Dr. Eiji Yamamoto for teaching me a lot of sincere advice about the experimental techniques necessary to conduct research in an unfamiliar field and great help for carrying out my research. I also wish to express appreciation to associate professor Dr. Haruno Murayama for giving me precise advice on the results of my experiments. I appreciate DIC Corporation for supporting me in terms of funding and the practical application of my research results. I would also like to express my gratitude to Kuraray Co., Ltd. for their cooperation in XPS measurements as well as in funding and practical application. Finally, special thanks are given to Ms. Uchida, the administrative assistant, and the members of the laboratory for their kind support of dairy laboratory life.

List of publication

Main articles

1. Convenient Unsymmetrical Disulfane Synthesis: Basic Zeolite-Catalyzed Thiol-Disulfane Exchange Reaction
   Eiji Yamamoto, Yasutaka Kawai, Kei Takakura, Moemi Kimura, Haruno Murayama, Hironobu Matsueda, Shujiro Otsuki, Hiroshi Sakata and Makoto Tokunaga
   ChemCatChem **2021**, *13*, 4694-4699. DOI: 10.1002/cctc.202101092

2. Aerobic Oxidation of Isoprene Glycol with Platinum-Bismuth Nanoparticles Supported on Metal Oxides
   Yasutaka Kawai, Keisei Sumikawa, Eiji Yamamoto, Haruno Murayama and Makoto Tokunaga
   (Under preparation)

Reference articles

1. Allenedicarboxylate as a Stereochemically Labile Electrophile for 1Chiral Organic Base-catalyzed Stereoselective Michael Addition
   Daisuke Uraguchi, Yasutaka Kawai, Hitoshi Sasaki, Kohei Yamada and Takashi Ooi
   Chem. Lett. **2018**, *47*, 594-597. DOI: 10.1246/cl.180031

Patents

1. 特願 2020-150754
   出願日：2020 年 9 月 8 日
   触媒の製造方法、及び触媒、並びに３－ヒドロキシ－３－メチルブタン酸の製造方法
   発明者：中山　修、徳永　信、村山　美乃、山本　英治、河合　靖貴、川田　真衣
   出願人：株式会社クラレ、国立大学法人九州大学

2. 出願番号：特願 2022-024040
   出願日：2022 年 2 月 18 日
   硫化オレフィンの製造方法
   発明者：松枝　宏尚、坂田　浩、大槻　周次郎、山本　英治、徳永　信、村山　美乃、髙城　悠太、河合　靖貴、高倉　慶、木村　萌水
   出願人：ＤＩＣ株式会社、国立大学法人九州大学